NASA
Technical
Paper
2735

September 1987

Frequency Domain Laser Velocimeter Signal Processor

A New Signal Processing Scheme

James F. Meyers and
James I. Clemmons, Jr.

NASA

NASA Technical Paper 2735

1987

Frequency Domain Laser Velocimeter Signal Processor

A New Signal Processing Scheme

James F. Meyers and
James I. Clemmons, Jr.

Langley Research Center
Hampton, Virginia

National Aeronautics
and Space Administration

Scientific and Technical Information Office

Abstract

A new scheme for processing signals from laser velocimeter systems is described. The technique utilizes the capabilities of advanced digital electronics to yield a "smart" instrument that is able to configure itself, based on the characteristics of the input signals, for optimum measurement accuracy. The signal processor is composed of a high-speed 2-bit transient recorder for signal capture and a combination of adaptive digital filters with energy and/or zero crossing detection signal processing. The system is designed to accept signals with frequencies up to 100 MHz with standard deviations up to 20 percent of the average signal frequency. Results from comparative simulation studies indicate measurement accuracies 2.5 times better than with a high-speed burst counter, from signals with as few as 150 photons per burst.

Introduction

A laser velocimeter signal processor must be capable of determining the oscillation frequency contained in a randomly occurring Gaussian-shaped signal burst generated by a particle passing through the laser velocimeter fringe pattern. The number of oscillations contained in a burst depends on the laser velocimeter optical system and the particle trajectory through the fringe pattern. The signal strength and signal-to-noise ratio of the burst oscillations depend on the optical system as well as the characteristics, velocity, and trajectory of the particle. Three measurement techniques are used to measure the frequency of these oscillations and thus the particle velocity ($V_p = L_f f_s$). The first approach is based on radar and radio technology and resulted in the development of the wideband frequency tracker in 1969 (refs. 1 and 2). The second approach, developed by several researchers beginning in 1971 (refs. 3, 4, and 5), is based on the direct measurement of time for a fixed number of oscillation cycles using counting techniques. The third technique, based on burst radar technology coupled with photon correlation spectroscopy, resulted in the development of the photon correlator in 1972 (ref. 6).

The merits of each approach have been determined and the choice of technique depends more on the application than on any fundamental superiority. The frequency tracker has proven to be an excellent signal processor where near-continuous signals are present, as in liquid flow measurements. However, the dependence of the tracker on measurement history limits the maximum slew rate, and its signal locking requirements make it unacceptable in most gas flow measurement applications because of both the high-frequency content of the flow turbulence and the typically low seeding rates. The high-speed burst counter is the most widely used technique, since it measures the oscillation frequency contained in a single burst independent of past history. Since this technique measures individual signal bursts, it is the ideal technique for gas flow applications where turbulence amplitude and spectral bandwidth can be large and seeding is sparse. The photon correlator has provided measurements of mean flow velocity from the photon-resolved signal bursts obtained in low signal amplitude applications. Although this technique provides little information on flow turbulence, it can make measurements from much lower signal levels than the other techniques.

With no new signal processing techniques being proposed since 1972, one would expect that this was a mature research area. Although these three techniques provided researchers with valuable fluid dynamics information, they have basic limitations. These limitations include a signal frequency limit on the minimum turbulence intensity amplitude that can be measured, and the subjective setting of the instrument parameters that affect measurement accuracy. Even with the improvements in technology since the techniques were first proposed, these limitations have not been reduced substantially. Therefore a new approach is proposed that utilizes a transient recorder to capture a signal burst and digital signal processing to determine its oscillation frequency. This approach should remove the frequency dependence on the measurement of turbulence intensity while reducing the minimum signal level for accurate measurements by a factor of five. The stability of the technique, along with the use of advanced digital control technology, should result in a "smart" instrument capable of configuring itself to maximize measurement accuracy based on the characteristics of the signals being measured. The present paper describes the proposed signal processor and presents the results of a comparative investigation between the high-speed burst counter and the proposed signal processor to determine the relative merit of the new processor.

Symbols and Abbreviations

ADC	Analog-to-digital converter
AFC	Automatic frequency control
AGC	Automatic gain control
DAC	Digital-to-analog converter
F	Mean signal frequency, Hz

FDLVSP	Frequency domain laser velocimeter signal processor
FFT	Fast Fourier transform
f_c	Digital bandpass filter center frequency, Hz
f_r	Reference clock frequency, Hz
f_s	Signal frequency, Hz
f'	Standard deviation of signal frequency, Hz
L_f	Fringe spacing, $L_f = \lambda/(2\sin(\theta/2))$, m
LSB	Least significant bit
MSB	Most significant bit
MSD	Most significant digit
U	Mean U-component (orthogonal to fringes) velocity, m/s
u'	Standard deviation of the U-component velocity, m/s
u'/U	Local flow turbulence intensity
VCO	Voltage controlled oscillator
$V_{\max}$	Maximum amplitude of a signal burst, V
$V_{\min}$	Signal burst amplitude one-half cycle from $V_{\max}$, V
V_p	Velocity of a seed particle passing through the fringes, m/s
θ	Angle between the crossing laser beams, deg
λ	Wavelength of laser light, m

Present Technology

As a small particle passes through the laser velocimeter fringe pattern in the sample volume (fig. 1), it will scatter light whose intensity will oscillate corresponding to the position of the particle in the alternating light and dark regions of the fringe pattern. A portion of this scattered light is collected by the receiving optical system and directed to the photocathode surface of a photomultiplier. The output electronic signal from the photomultiplier is composed of a collection of Poisson distributed photoelectrons whose average occurrence rate is proportional to the instantaneous light intensity at the photocathode. As the intensity increases from the photon-resolved regime, i.e., one photon per response time of the photomultiplier, the additional photon arrivals add together and increase the output signal current. With sufficient photons, the signal approaches a Gaussian-shaped signal burst containing the oscillation frequency (fig. 2). The primary goal of a laser velocimeter signal processing technique is to determine the oscillation frequency contained in the burst. The three techniques currently used are the wideband frequency tracker, the high-speed burst counter, and the photon correlator.

Wideband Frequency Tracker

The wideband frequency tracker measures the oscillation frequency based on technology derived from Doppler radar and FM radio receivers. As shown in figure 3, the input signal is electronically mixed with a reference signal to yield a difference signal whose frequency is located within the bandwidth of an electronic frequency discriminator (frequency-to-voltage converter). When the reference frequency is properly set, the average mixed signal frequency matches the center of the discriminator. The discriminator then yields an output signal that is 0 V with instantaneous variations in the output voltage proportional to instantaneous differences between the instantaneous incoming signal frequency and the reference frequency, and thus demodulates the FM signal. If the discriminator output is low-pass filtered and used as a nulling control signal in the adjustment of a voltage-controlled oscillator (VCO), an automatic frequency control (AFC) circuit is obtained, which "locks" in the average radio signal frequency and removes the effect of frequency drift.

The wideband frequency tracker uses a ramp voltage function to scan its input frequency band until it locates the laser velocimeter signal frequency and locks on to it with the AFC. Monitoring the control signal to the VCO provides a measure of the average signal frequency, and monitoring the output from the discriminator provides a measure of the instantaneous signal frequency deviations about the average. Combining the two signals, with proper amplification to equate the calibrations, provides an instantaneous measure of the signal frequency.

In liquid flow studies this technique works extremely well, since the particle number density is naturally high enough to yield an almost continuous series of signal bursts. However, when used in gas flow studies the particle number density is considerably less, which yields many "holes" in the time history of the signal. To overcome this problem, the original trackers used analog feedback circuitry to provide a holding signal to keep the VCO control signal constant for a short time before a loss of "lock" sends the tracker back to the ramp scan mode. Even

this control required that a signal burst be present at least 15 percent of the time, which translates to a data rate of 75 000 particles per second passing through the sample volume of a typical system at a flow velocity of 100 m/sec. Digital control technology has since reduced the required time a burst must be present to 1 percent, e.g., 5000 particles per second at 100 m/sec. Even this rate is still too high for most wind-tunnel applications.

A secondary problem with the wideband frequency tracker is the limit on the maximum frequency deviation and its rate of change. For example, a typical tracker can operate with a range within the voltage ramp function from 1 MHz to 10 MHz with a discriminator bandwidth of 0.63 MHz and a maximum slew rate of 58 MHz/msec. If the flow turbulence is Gaussian in its probability density function, the maximum turbulence that can be measured is 4.2 percent for an average signal frequency of 5.0 MHz before clipping occurs at ± 3 standard deviations. Since flow reversal occurs at a standard deviation of 20 percent, the capabilities of the tracker are approximately a factor of 5 below desired characteristics. The effect of the slew rate can be found if it is assumed that the flow oscillates in a sinusoidal fashion ± 0.315 MHz about an average signal frequency of 5.0 MHz. The slew rate limit of 58 MHz/msec limits the maximum frequency of the sine function to 46 kHz.

High-Speed Burst Counter

The approach used in the high-speed burst counter technique is much simpler than the frequency tracker approach. The counter technique detects the onset of a signal burst and measures the time required for nth zero crossings of the pedestal-removed signal. The technique, illustrated in figure 4, begins by bandpass filtering the incoming signal. A high-pass section removes the pedestal voltage, and a low-pass section increases signal-to-noise ratio by limiting the noise bandwidth. The filtered signal then passes through a double threshold/zero crossing detector circuit that converts it to a square wave signal. This signal passes to a 4-bit counter that controls two high-speed counters. When the first signal pulse occurs, the two high-speed counters and both count gates are reset to arm the system. The second pulse opens both count gates and the two high-speed counters begin counting reference clock pulses. When the seventh pulse occurs, the 5-count gate is closed. Its corresponding high-speed counter now contains the number of reference clock pulses occurring within five cycles of the signal burst. When the tenth pulse occurs, the 8-count gate is closed along with its corresponding high-speed counter containing the number of reference clock pulses occurring within eight cycles of the signal burst. The tenth pulse also triggers the 5:8 count comparison circuit, which compares the reference clock counts contained in the two high-speed counters for a comparison within the selected (from panel control) accuracy. If the comparison is within the selected accuracy, the 5:8 count comparison circuitry outputs a data-ready pulse to the external data acquisition system, commanding it to read the data contents of the 8-count high-speed counter.

The advantages of the high-speed burst counter are (1) a measurement is completed during the signal burst, (2) an output is obtained only when a measurement has been made, (3) measurements are independent of previous history, and (4) the time of occurrence may be determined by measuring the time between data-ready pulses. The disadvantages include (1) a residual f'/F results from the effects of signal-to-noise ratio on the determination of the first and the nth zero crossings, and from time quantization by the reference clock (an input signal with $f'/F = 0$ will yield a measurement $f'/F > 0$), and (2) the possibility of serious measurement errors if the filter and threshold settings are chosen improperly.

Photon Correlator

The simplest technique, photon correlation, autocorrelates the input signal during the measurement time. The input signal is digitized by using a single-bit comparator to yield a pulse train that is autocorrelated by a single-bit correlation circuit. The multiplying circuits within the correlator consist of a simple series of logic AND gates (fig. 5) for increased speed and thus increased input signal bandwidth. The advantage of this technique is that correlation increases the signature of the "average" signal burst while removing the uncorrelated photomultiplier shot noise. The disadvantages are (1) no turbulence quantities are available, since only the "average" frequency can be measured; (2) flow turbulence decreases the number of cycles in the correlation function and thereby decreases accuracy; and (3) amplitude quantization of the input signal by the single-bit comparator increases the effect of noise on the correlogram in conditions in which the signal amplitude and/or visibility $\{ (V_{max} - V_{min}) / (V_{max} + V_{min}) \}$ vary, e.g., in polydisperse particle size environments such as the atmosphere.

The Ideal Signal Processor

An ideal laser velocimeter signal processor would combine the advantages of these three techniques while eliminating their limitations. From the wideband frequency tracker technique, the processor would use the ability to follow frequency variations of the average signal (automatic frequency control AFC) and to maintain a constant signal level (automatic gain control AGC). The high-speed burst counter technique would contribute the ability to complete the signal frequency measurement during the signal burst. Finally, the photon correlator technique would contribute the ability of being insensitive to input signal-to-noise ratio down to the photon-resolved regime.

The remainder of the present paper addresses an attempt to combine these abilities into a new type of signal processor and to demonstrate its capabilities based on computer simulations of input signal bursts and processing algorithms. It will be shown that although the ideal processor was not realized, the new signal processor should have much improved capabilities and accuracies than present technology.

Frequency Domain Laser Velocimeter Signal Processor

Overview

The design studies of the frequency domain laser velocimeter signal processor began by evaluating the characteristics of laser velocimeter signal bursts and by looking at the elements of each of the present signal processing techniques. The evaluation indicates that the signal bursts are of short duration and obey Poisson occurrence statistics with very low average rates. The signal amplitudes have little variation if the particles are all approximately the same size. The turbulence intensity parameter f'/F must not be allowed to exceed 20 percent to prevent frequency aliasing at 0 Hz.[1] The desirable elements from the frequency tracker include the automatic gain control circuitry and the automatic frequency control circuitry, but analog loop restrictions prevent single signal burst detection. The ability of the high-speed burst counter to measure single signal bursts is a desirable element, but its sensitivity to signal-to-noise ratio and time quantization is undesirable. The insensitivity to signal-to-noise ratio of the photon correlator is desirable, but the inherent need for multiple signal bursts is not.

[1] When u'/U is greater than 20 percent, a Bragg cell is used to bias the signal frequency away from 0 Hz; thus f'/F is reduced below 20 percent.

Studies indicate that a signal processor is usually waiting for a signal burst to arrive. If the presence of the signal burst can be detected and the waveform captured and stored in a digital memory, ample time would be available for processing prior to the arrival of the next signal burst. This forms the basic strategy of the proposed signal processor: a high-speed burst capture circuit followed by signal analysis circuitry furnishing data to digital feedback loops for gain and average frequency adjustments and for the measurement of the oscillation frequency in each signal burst.

Although the signal bursts are digitized by the other techniques, the only true multibit digitization of signal bursts has occurred by using transient recorders (ref. 7) with computer processing of the captured bursts. The major advantage of the transient recorder is the ability to capture the entire burst without the assumption of symmetry or high signal visibility as in the other techniques. A secondary advantage of the transient recorder is its maintenance of amplitude information which could be input to circuitry for controlling signal amplification. The disadvantages of a transient recorder, however, are manual setting of signal amplification and sampling rate, and the slow transfer of the data to the external computer. If these problems can be overcome, this approach would seem to have a distinct advantage over classical laser velocimetry signal processing.

If a transient recorder can be designed to operate in the manner of a shift register with the digitized signal continuously passing through the recorder, the contents can be continuously interrogated to detect a signal burst. When a signal burst has been found, the shifting process would be halted and the data transferred to data latches to provide the input to the signal processor section. This technique allows processing the laser velocimeter output only when signal bursts are present. By using the amplitude and frequency information obtained from the signal burst, the amplification and sampling rate can be adjusted to maximize measurement accuracy. In practice, the system should not adjust the sampling rate while acquiring data, since this would require the output of the rate along with the desired measurement information. Thus the system should be designed to operate in two phases, a setup phase to establish the sampling rate and a data acquisition phase with the rate held constant. The information on signal amplitude can be used to continuously control an automatic gain circuit to keep the signal amplitude within the optimum bounds. This basic approach is illustrated in the block diagram in figure 6.

Although it would appear that the most straightforward approach to determine the oscillation

frequency of the captured signal burst would be to perform a fast Fourier transform (FFT) and to determine the location of the peak, this approach is not necessarily the most efficient for laser velocimeter signal burst processing. The FFT performs many unnecessary calculations to determine the energy distributions for frequencies above and below the oscillation frequency, since it calculates the entire frequency spectrum. It would be much more efficient if only those frequencies surrounding the oscillation frequency were investigated. This ideal can be realized by using a digital bandpass filter bank with control of the sampling frequency during the above-mentioned setup phase to approximate the desired Fourier energy calculations. By using $f'/F = 20$ percent and ± 3 standard deviations, 99.73 percent of the energy contained in a Gaussian frequency (velocity) distribution will be obtained for the maximum measurement conditions. Therefore, a bank of seven digital bandpass filters, each with a bandwidth of at least $f'/F = 0.2$ and a center frequency separation of $0.2f_r$, can be used to obtain the equivalent energy distribution as an FFT with an increase in computational speed (fig. 7).

The use of digital bandpass filters offers several signal processing possibilities. The peak of the energy distribution passing through the filter bank can be determined by using curve fit or statistical procedures to yield the oscillation frequency. The filter passing the greatest energy for a given signal burst could be used as a narrow bandpass filter for a high-speed burst counter. The signal-to-noise ratio may be increased for low f'/F by changing the coefficients of the filters to reduce both the bandwidth and the frequency spacing. These possibilities may even be combined by using a control algorithm designed to maximize measurement accuracy of the input signals.

A frequency domain laser velocimeter signal processor was proposed which uses this measurement strategy with microprocessor control and an optimizing control algorithm. This processor operates without operator intervention from the photon-resolved regime to high signal levels, with an upper signal frequency limit of 100 MHz for signal bursts containing 20 cycles within the $1/e^2$ amplitude limits. This processor would be composed of a transient recorder with unfiltered automatic gain amplification, analog-to-digital conversion, shift register storage, and burst detection circuitry; and a computational signal processor including a bank of seven adaptive digital bandpass filters, and energy detection, zero crossing detection, and automatic frequency control algorithms. The processor would use the techniques of automatic frequency control and automatic gain control from the wideband frequency tracker while eliminating the slew rate errors and time-of-flight broadening. It would have the ability to measure the frequency of a single signal burst while eliminating filter bias and quantizing errors present in the high-speed burst counter technique. Finally, the processor, like the photon correlator, would be relatively insensitive to the signal-to-noise ratio of the input signal burst yet not have the correlation phase errors due to improper pedestal removal. The overall system function diagram is shown in figure 6 and with increased detail in figure 7. Detailed descriptions of the circuit elements and their operation follow.

Analog-to-Digital Converter

The signal bursts obtained from a laser velocimeter (fig. 2) have two structural components: a pedestal voltage due to the Gaussian light intensity profile of the laser beams, and an oscillating voltage due to the constructive and destructive interference between the two crossing laser beams yielding the fringe pattern (ref. 4). The signal amplitude at the output of the photomultiplier can vary from single photon levels (typically 2 mV) to full saturation (typically 1.5 V). The amplitude ratio, or signal visibility $\{ (V_{\max} - V_{\min}) / (V_{\max} + V_{\min})$ at the center of the signal burst$\}$, between the oscillating voltage and the pedestal voltage can vary from zero to unity, depending on the light scattering characteristics of the particle and the configuration of the laser velocimeter optical system. Typical systems yield signals with amplitudes of approximately 0.4 V and visibilities between 0.5 and 1.0. The analog-to-digital converter (ADC) is required to have sufficient resolution to provide both frequency and amplitude information for inputs to the AFC and AGC circuitry over a range of signal amplitude and a range of visibility.

The design of the ADC includes the choice of the number of bits and the triggering voltage levels of the comparators. A single-bit ADC can provide frequency information if the signal visibility is high, but cannot provide amplitude information. A 2-bit ADC can provide both frequency and amplitude information if the triggering voltage levels are chosen properly. If the peak signal amplitude is 1.5 V, the corresponding minimum in the visibility function is 0.0 V for a visibility of 1.0, 0.5 V for a visibility of 0.5, 0.64 V for a visibility of 0.4, 0.808 V for a visibility of 0.3, etc. By choosing the highest triggering voltage level in the ADC to be 0.8 V, saturation signals with visibilities down to approximately 0.3 could be measured. Dividing 0.8 V into three uniformly spaced triggering voltages yields 0.8-V, 0.5333-V, and 0.2667-V levels. For signal bursts containing 20 oscillations within the

$1/e^2$ voltage levels, this ADC will yield a digital waveform containing 18.6 cycles at a peak voltage of 1.5 V and 8.2 cycles at a peak voltage of 0.375 V to yield a 4:1 input voltage spread of signal bursts with visibilities down to approximately 0.3. If a nonuniform triggering voltage spacing is used, e.g., 0.8 V, 0.4 V, and 0.2 V, the same accuracies in amplitude and frequency resolution would be obtained, but the number of digitized cycles would increase to 20.0 for an input signal of 1.5 V and 11.2 for an input signal of 0.375 V.

Other ADC's were tested, with 3- and 4-bit ADC's providing less than a 0.01-percent increase in measurement accuracy over the 2-bit ADC. The final signal processor was therefore designed with the 2-bit configuration and the nonuniform spacing of triggering voltage levels of 0.2 V, 0.4 V, and 0.8 V (fig. 8) to decrease circuit complexity and increase measurement signal cycle count.

Shift Registers

The temporary storage element in the transient recorder section consists of a pair of 256 × 1-bit shift registers to acquire the 2-bit output from the ADC. The use of shift registers allows the system to monitor the laser velocimeter output continuously and to latch the register contents only when it has been determined that a signal burst is contained in the shift registers. This technique removes the requirement for processing the input signal continuously. Further, since the arrival rate for the signal bursts is in the kHz range or less in gas flow applications, real-time signal processing is not necessary. The signal burst should be processed prior to the arrival of the next burst.

The design goal of measuring oscillation frequencies up to 100 MHz from signal bursts containing 20 cycles within the $1/e^2$ amplitude levels establishes the desired performance level of the transient recorder. At present, GaAs digital circuitry is available that can operate in the region of 1.0 GHz to yield a maximum digitizing rate of 10 samples per cycle at oscillation frequencies of 100 MHz. Thus the shift register must be 200 bits in length to hold the 20 cycles of the design signal burst, provided that the burst is centered within the registers. The final design shift registers were chosen to be 256 bits in length to help ensure capture of the total burst and to provide for signals with oscillation frequencies below the average.

The speed requirements for the shift registers may be reduced below the maximum 1.0 GHz sampling frequency by using decoders to operate several small shift register circuits in a parallel scheme. This technique is possible since electronic logic circuits normally trigger on the edge of a clock pulse but require a certain time for circuit stabilization. This time may be obtained by passing the next clock pulse to other circuits, with the total loop time being longer than the stabilization time for each circuit. A schematic diagram illustrating this scheme as applied to the signal processor is given in figure 9.

Signal Burst Detection Circuit

With the completion of the acquisition section design, the control circuitry necessary for recognizing the presence of a signal burst in the shift registers must be designed. Two concepts typically used for signal detection are threshold triggering and energy detection. The energy detection scheme is more attractive for use with the 2-bit ADC as it does not require the fine measurement amplitude resolution of the threshold trigger method. A simple energy detection circuit can be constructed by using an up-down counter, with the input to a shift register controlling the up count and the data leaving the register controlling the down count (fig. 10). It is sufficient to monitor just the MSB shift register, since the gain control circuitry is designed to keep the signal burst levels above the MSB threshold while the noise level is kept below the MSB threshold. Simulation test results have verified the operation of the circuit with signals containing as few as 70 photoelectrons per burst.

The number of occurrences of set bits within the MSB shift register depends on the signal burst amplitude, visibility ratio, and oscillation-to-clock-frequency ratio. The effects of the signal amplitude and the visibility ratio are illustrated in table I for the MSB value of 0.4 V and 10 samples per cycle, as chosen previously as a test example.

Table I. Count Values in Signal Burst Detection Circuit for Various Signal Burst Amplitudes and Visibilities for MSB Set to 0.4 V

Signal amplitude, V	Count values for visibility ratio of—			
	1.0	0.5	0.4	0.3
1.5	87	127	137	143
1.0	59	77	99	107
.75	46	57	63	75
.5	17	17	19	25
.375	0	0	0	0

The results presented in the table indicate that the count of set bits in the MSB shift register decreases

with decreasing signal amplitude but increases with decreasing visibility. The table also indicates that a threshold count of 16 would detect signal bursts above 0.5 V with visibilities above 0.3.

As a second test sample, the MSB value was chosen to be 0.2 V, which yields the results in table II.

Table II. Count Values in Signal Burst Detection Circuit for Various Signal Burst Amplitudes and Visibilities for MSB Set to 0.2 V

Signal amplitude, V	Count values for visibility ratio of—			
	1.0	0.5	0.4	0.3
1.5	123	173	181	185
1.0	101	147	155	159
.75	87	127	137	143
.5	59	77	99	107
.375	46	57	63	75

These results show that an increase in the dynamic range of signal detection from 3:1 to 4:1 with a higher set bit count will help in rejecting random counts from noise. Since a decrease in the ADC triggering threshold values will not affect measurement accuracy, they were lowered to 0.4 V, 0.2 V, and 0.1 V to increase the dynamic range of signal detection and to increase the detection count to 32.

The remaining design concern for the signal burst detection circuit is the effect of signal oscillation frequency on the dynamic range. As the oscillation frequency increases, the number of samples above the MSB decreases. For example, if the signal oscillation frequency increases by 20 percent, the number of samples per cycle reduces from 10 to 8, which reduces the values in the above table by 20 percent. To continue this trend, the design requirement of measuring signal oscillation frequencies ± 3 standard deviations of $f'/F = 20$ percent reduces the values in the above table by 60 percent. Thus signal bursts with peak voltage values of 0.5 and below will not be detected; again the dynamic range of the system is compressed. This problem can be corrected by automatic control of the amplification circuitry.

Automatic Gain Control Circuitry

The narrow dynamic range of the signal burst detection circuitry requires automatic gain control on the input amplifiers of the transient recorder. Total amplification should not, however, be automatically controlled to keep the system from amplifying the background noise between signal bursts into the detection range. Thus a scheme of a small range automatic gain control amplifier coupled with a manually controlled amplifier is chosen to obtain the full dynamic range from single photon detection to photomultiplier saturation.

It was found in the previous section that the signal burst detection circuitry directly detects signal bursts with peak voltage values of 1.5 V, or photomultiplier saturation. Thus signal bursts of this level require no amplification, i.e., a gain of unity. Photon-resolved signal bursts have output signal levels of approximately 0.002 V and require amplification to levels above the detection threshold, e.g., a gain greater than 100. The choice was an amplification system with binary steps, i.e., 1, 2, 4, 8, etc., and a manually controlled amplifier to provide the nominal gain, with the AGC amplifier controlling gain between adjacent amplification steps. For example, if the manually controlled amplifier was set to a gain of 4, the coupling of the AGC amplifier would yield a total gain from 2 to 8. This is accomplished with a manually controlled amplifier gain of 2 (not the setting of 4) and an AGC amplifier range from 1 to 4. Therefore, with the amplification system providing gains from half to twice the selected value, the input dynamic range has been increased sufficiently to allow the detection of low level and high oscillation frequency (few samples per cycle) signal bursts.

A signal integration scheme similar to the signal burst detection circuitry will yield the control information from the signal bursts. If the control signal was the output from the highest trigger threshold comparator in the ADC, an estimate of the peak signal burst voltage could be obtained. This signal, which is easily obtained by ANDing the signals going to the two shift registers to yield the most significant digit (MSD), is used to control the up input of an up-down counter. Likewise, the data leaving the two shift registers are ANDed and used to control the down input. When a signal burst has been detected by the signal burst detection circuitry, a delay of 64 reference clock pulses is started to allow better centering of the signal burst within the shift registers to yield a better waveform for the estimate of the amplitude. Following the delay, the reference clock is halted to stop the transient recorder in order both to transfer the shift register contents to temporary storage registers for signal processing and to allow interrogation of the contents of the AGC counter for the adjustment of amplification, if necessary.

The AGC circuit should respond slowly to changes in signal burst amplitude to minimize short-term effects in amplitude due to particle characteristics and flow fluctuations, while providing

adjustment for long-term variations in signal level due to changes in the collection optics of the velocimeter, particulate coating of viewing windows, etc. The AGC must provide sufficient gain for signal bursts of a given amplitude to be detected regardless of the oscillation frequency (within ±60 percent of the nominal average oscillation frequency) and must decrease gain for signals with low signal visibility to put the oscillations within range of the triggering thresholds of the ADC. For example, from table II a signal burst with a peak amplitude of 0.5 V and a visibility of 1.0 can be detected, but a burst with an oscillation frequency 60 percent higher will yield only a count of 23 and not be detected, which biases the data toward lower frequencies. A signal burst with a peak amplitude of 1.5 V and a visibility of 0.5 will be detected, but its center cycle, with a minimum of 0.5 V, will not cross the upper triggering threshold of 0.4 V and yield a measurement error. The first example should have an increase in amplification whereas the second should be decreased. By expanding table II to include minimum center voltage, MSD count, and detection count for a sampling rate of 4 per cycle, the choice of gain adjustment counts may be obtained as shown in table III. Those entries in table III with an ↓ must be lowered in amplification because the minimum voltage of at least the center cycle is above the MSD triggering level and the cycle will be missed. Those table entries with an ↑ must be further amplified because signal bursts digitized at 4 samples per cycle will be below the detection threshold of 32 counts. This example indicates that signal bursts yielding MSD counts of 99 or greater should have the amplification reduced, and those yielding MSD counts of less than 32 should have the amplification increased. Choosing the MSD up-down counter to be 7 bits in length allows the upper two bits to be used as control signals to set the lower threshold to 31 counts and the upper threshold to 96. These two control signals are ANDed together with the delayed signal detection pulse to provide a down-count signal to the AGC amplification counter (fig. 10). Conversely, the inverses of the two control signals are ANDed together with the delayed signal detection pulse to provide the up-count signal. Thus if the two upper bits of the AGC counter are high (a value of 96 or greater indicated) the amplification counter will be decremented; if the bits are both low (a value less than 32 indicated) the amplification counter will be incremented. The value contained in the amplification counter would drive a digital-to-analog converter used to provide a drive voltage to a combination of light emitting diode (LED) and photo resistor used as the feedback resistor of an

Table III. Count Values for AGC Counter of MSD Signals and Respective Counts Above Detection Threshold for 10 and 4 Samples Per Cycle and Minimum Center Cycle Voltage

Visibility ratio	Signal amplitude, V	Minimum center cycle voltage, V	Count values for 10 samples per cycle	MSD	Count values for 4 samples per cycle	Indicated gain adjustment
1.0	1.5	0	123	87	49	
↓	1.0	↓	101	59	40	
↓	.75	↓	87	46	34	
↓	.50	↓	59	17	23	↑
↓	.375	↓	46	0	17	↑
0.5	1.5	0.5	173	127	69	↓
↓	1.0	.33	147	77	59	
↓	.75	.25	127	57	51	
↓	.50	.167	77	17	31	↑
↓	.375	.125	57	0	23	↑
0.4	1.5	0.64	181	137	72	↓
↓	1.0	.43	155	99	62	↓
↓	.75	.32	137	63	55	
↓	.50	.21	99	19	40	
↓	.375	.16	63	0	25	↑
0.3	1.5	0.81	185	143	74	↓
↓	1.0	.54	159	107	64	↓
↓	.75	.40	143	75	57	
↓	.50	.27	107	25	43	
↓	.375	.20	75	0	30	↑

operational amplifier. As the count within the amplification counter increases, the voltage to the LED increases, which decreases its brightness and increases the resistance of the photo resistor and thereby increases the gain of the amplifier and completes the AGC loop. By using a 4-bit amplification counter, the amplifier gain range from 1 to 4 is divided into units of 0.1875 to provide the desired slow response AGC. A schematic of the AGC circuit along with the signal burst detection circuit is shown in figure 10.

Data Processing Circuitry

Once the signal burst is centered in the shift registers, the reference clock halted, and the data transferred to temporary data latches, the captured signal burst may be analyzed to determine its oscillation frequency. The latched data are placed on a common input data bus to a parallel bank of seven digital, elliptic bandpass filters. The center frequencies and bandwidths of the digital filters are selected as fractions of the reference clock or sampling frequency. For example, the center frequency of the center filter is set to a value of $f_c = 0.10f_r$, or 10 samples per cycle, the next lower filter is set to $f_c = 0.08f_r$, or 12.5 samples per cycle, etc. If the reference clock were set to 100 MHz, an input signal burst with an oscillation frequency of 10 MHz would pass through the center filter and be attenuated by the other filters to yield an energy distribution following the filter bank that is symmetric and peaked in the center. A signal burst with an oscillation frequency of 12 MHz would pass through the next higher filter (fifth filter with 8.3 samples per cycle) to yield an energy distribution peaked at the fifth filter. If the reference clock were increased to 125 MHz, the 12 MHz oscillation frequency would then pass through the center filter. Therefore the same filter bank is used over the entire range of the processor, with the range setting established by the value of the reference clock frequency, yet each filter has the same relative bandwidth.

Elliptic filters were chosen because they yield the sharpest cutoffs and the flattest passband yet require the fewest computations of the standard filter types. The filter spacing was chosen to be $0.02f_r$ to correspond to the design requirement to measure $f'/F = 20$ percent. Seven filters are used to provide the ± 3 standard deviations necessary to capture 99.7 percent of the signal bursts when $f'/F = 20$ percent. Therefore the center frequencies of the filter bank are $0.04f_r, 0.06f_r, 0.08f_r, 0.10f_r, 0.12f_r, 0.14f_r$, and $0.16f_r$. The energy distribution passing through the filter bank is measured by using a square-law detector-accumulator circuit following each of the seven filters. When the captured signal burst passes through the filter bank, the oscillation frequency can be determined by curve fitting the integrated energies contained in the seven accumulators.

Extensive simulation studies were conducted by using Monte Carlo modeling of the input signal bursts (ref. 8) and a model of the transient recorder and signal processor with all control functions to optimize the design of the data processing circuitry. The starting design configuration used the seven digital filters of the $0.02f_r$ spacing without bandwidth overlap of adjacent filters. The simulation studies of this design indicated that ensemble mean measurement errors were in the 5-percent range with residual f'/F (measured f'/F with an input $f'/F = 0$) error of approximately 0.6 percent. The measurements of ensemble average and standard deviation were found to be constant until the input f'/F reached 3 percent, which indicated that energy was not passing through adjacent filter bandwidths. The design configuration was modified to increase the overlap of adjacent filters, with iterations until the optimum overlap of 40 percent was found. For example, the digital filter with a center frequency of $0.08f_r$ has its upper break point located at $0.094f_r$ and the upper adjacent filter ($0.10f_r$) has its lower break point located at $0.086f_r$. The resulting configuration reduced the ensemble mean measurement errors to the 3-percent range with the same residual f'/F. Trends of input f'/F above the residual level were also tracked. A further improvement (ensemble measurement errors to 2 percent) was found by determining the oscillation frequency from a binomial curve fit of just the three energy measurements at or adjacent to the peak.

Apparently the difficulties in obtaining good measurement accuracies with the energy detection approach were due to the narrow spectral bandwidth (frequency bandwidth due to the finite number of cycles within the signal burst) of the energy within the signal burst as compared with the spacing of the filters. Thus, most of the energy passed through a single filter, with the overlap into adjacent filters yielding only a small fraction of energy, a level comparable to the noise of the digital filter–energy detection process. Further modifications of this scheme would compromise the desired measurement specifications.

Another approach for determining the oscillation frequency would be to use the digital filter bank as a series of adaptive narrow bandpass filters providing signal conditioning for a high-speed burst counter. This scheme would provide a more accurate frequency measurement and an increased signal-to-noise ratio than a standard high-speed burst counter, since the filters have narrower bandwidths.

Zero crossing detection accuracy is increased by interpolating the captured signal burst waveform to eliminate quantizing errors. The required circuitry can be much simpler than the high-speed burst counter circuitry because the transient recorder performs the detection function normally performed by the double threshold detector of the counter and the 5:8 count comparison. The scheme consists of a single negative threshold arming circuit that triggers a zero crossing detector to yield measurements of crossings with positive slopes of the filtered signal burst. When a zero crossing is detected, the exact location is estimated by straight line interpolation between the last negative value and the first positive value, with the result stored in memory. A zero crossing detector circuit is placed behind each of the seven filters (fig. 11). When the signal burst has passed through the filter bank and has been processed by the zero crossing detectors, the energy distribution is determined and the zero crossing detector memory for the filter passing the greatest energy is interrogated. The first two and the last two zero crossing locations are rejected to remove discontinuities due to time clipping of the signal burst by the transient recorder. The remaining zero crossing locations are used to determine the oscillation frequency as a function of the sampling frequency.

The use of the zero crossing detection scheme reduced ensemble measurement errors to less than 0.3 percent with a residual f'/F of 0.4 percent independent of input frequency. These errors are an improvement over the high-speed burst counter, which has an ensemble measurement error of 0.4 percent over the input frequency range, but has a minimum residual f'/F of 0.4 percent at an oscillation frequency of 5.0 MHz, which increases up to a residual f'/F of 1.4 percent at an oscillation frequency of 100.0 MHz.

Although these errors are acceptable for measurements of high input f'/F, since they are typically less than the statistical uncertainties, they become more significant when the input f'/F decreases. If it can be determined that the input f'/F is low, the digital filter bank could be modified in real time by changing the computational coefficients to decrease the filter spacing and bandwidths to increase the signal-to-noise ratio of the filtered signal bursts. This can be accomplished during the setup phase with the automatic frequency control (AFC) yielding the estimates of the average oscillation frequency and standard deviation about the average.

During the setup phase, the AFC will adjust the reference clock frequency until the average oscillation frequency passes through the center filter or the next lower filter. If f'/F is less than 5 percent, all signal bursts will pass through these two filters. This frequency range could be spread over the seven filters by changing the parameters of the filter bank, thus their spacing and bandwidths would be changed. To carry this idea further, three sets of coefficients with center filter frequencies of $0.072f_r$, $0.088f_r$, and $0.10f_r$, with a spacing of $0.004f_r$, could be used to increase signal-to-noise ratio by 7 dB. The proper set of coefficients would be selected based on the estimate of the average frequency. With this approach, simulation studies were repeated for low values of f'/F, using both the zero crossing detector approach and the curve fitting of the energy distribution for signal processing. Both methods yielded similar results, with the ensemble measurement errors reduced to 0.1 percent and the residual f'/F reduced to 0.2 percent. The increase in accuracy of the zero crossing detection method is attributed to the increase in signal-to-noise ratio of the filtered signal, and the increase in accuracy of the energy distribution method is attributed to the greater energy overlap of the spectral bandwidth of the signal burst into the adjacent narrower filters. The final design uses the energy distribution approach for processing signal bursts when f'/F is less than 5 percent because this method allows the measurements to accumulate for increased accuracy of the average signal frequency for very low signal-to-noise ratios, i.e., few photons per burst.

Variable Reference Clock

The key element in providing an AFC capability for the system, which allows the digital filter bank to be held constant, is a variable frequency reference clock to control the sampling rate. This task can be accomplished by using three crystal oscillators at 1.0 GHz, 800 MHz, and 640 MHz, each coupled with a binary counter used as a frequency divider (fig. 12). This selection of frequencies yields a reference clock that allows the shift of the input oscillation frequency to the next higher filter with each decrease in clock frequency. For example, an input oscillation frequency of 50 MHz will pass through the lower two filters equally (25 and 16.7 samples per cycle) with a reference clock frequency of 1.0 GHz. As the reference clock frequency is lowered, the energy will pass through higher filters, e.g., 800 MHz clock yields filter 2 at 16.7 samples per cycle, 640 MHz yields filter 3 at 12.5 samples per cycle, 500 MHz yields filter 4 at 10 samples per cycle, etc. The desired reference clock frequency is selected by activation of the appropriate AND gate (fig. 12) by the microprocessor.

Once the desired frequency is selected, the signal is routed to the ADC, shift registers, signal detection circuit, and the AGC.

Typical System Operation

The frequency domain laser velocimeter signal processor (FDLVSP) is designed to have two phases of operation. The first phase is the instrument setup phase to select the optimum reference clock frequency and filter bank, and the second is the data acquisition phase. The following example is presented as an illustration of the operation of the system.

The external data acquisition system issues a command control pulse to the FDLVSP to begin the data acquisition process. The controlling microprocessor in the FDLVSP interprets this pulse as a "begin data acquisition" control and sets the reference clock to 1.0 GHz, loads the digital filter bank with the parameters to accept an f'/F of 20 percent, activates the zero crossing detection signal processing, and acquires the first signal burst to begin the setup phase (fig. 13). The oscillation frequency for the captured signal burst is determined, which yields the ratio of oscillation, or signal, frequency to reference frequency f_s/f_r. If the ratio is less than 0.08, the reference clock frequency is lowered by approximately 20 percent (equivalent to the frequency spacing between adjacent filters) and the next signal burst is acquired. This procedure is continued until the signal frequency becomes greater than 0.08; the microprocessor then locks the reference clock frequency. If during this portion of the setup phase the AGC circuit reaches a limit, the appropriate limit lamp is lit on the front panel and further acquisitions are suspended until the manual gain control is adjusted. The microprocessor then resets the system and begins the setup phase again.

The next 10 signal bursts are then acquired to calculate an estimate of the average signal frequency as an assurance that the microprocessor has locked the reference clock at the proper frequency to center the signal frequencies within the filter bank. If the average signal frequency calculated by the microprocessor is less than $0.08f_r$, the reference clock is lowered a further 20 percent and 10 more signal bursts are acquired and the check is repeated. If the ratio is greater than 0.12, the reference clock frequency would be raised 20 percent and the process repeated. This continues until the average signal frequency is within the bound from $0.08f_r$ to $0.12f_r$. This procedure is necessary to ensure the centering of the data for large standard deviations of signal frequency. Again, if the AGC circuit reaches a limit, the manual gain must be adjusted and the setup phase restarted.

The setup phase continues by acquiring the next 30 signal bursts and by calculating both the average and the standard deviation, provided the AGC does not reach a limit. If the calculated f'/F is less than 5 percent, the microprocessor loads the filter bank with the appropriate narrow bandwidth filter parameters based on the average signal frequency, deactivates the zero crossing detectors, and activates the energy distribution processor. When the coefficients, if required, are loaded into the filter bank, the microprocessor places the appropriate code indicating the frequency of the reference clock on the output data bus and flags the external data acquisition system to accept the data word. This transfer completes the setup phase and begins the data acquisition phase.

When the next signal burst is acquired, the signal detection control pulse is routed through a delay counter (to allow sufficient time for signal processing) to be used as the flag for the external data acquisition system to indicate that data are available for transfer. The data acquisition phase continues until a command control pulse fails to arrive from the external data acquisition system within 10 msec following the issue of a flag pulse; the FDLVSP then times out in an end-of-data-acquisition state. Receipt of the next command control pulse will be interpreted as a "begin data acquisition" control and will initiate a new data acquisition cycle beginning with the setup phase.

The external computer system completes the data acquisition process by converting the measured frequency fractions to absolute frequency values by multiplying the measurements by the reference clock frequency obtained from the coded value contained in the first data word. These results are then converted to velocity by multiplication of the array with the laser velocimeter fringe spacing. Interarrival times, or time between adjacent signal bursts used for turbulence power spectra measurements (ref. 9), are obtained by measuring the time between the flag pulses from the FDLVSP in the same manner as with the high-speed burst counter.

Photon-Resolved and Laminar Flow Signal Processing

If the laser velocimeter signals are photon resolved because of optical system limitations, the frequency domain laser velocimeter signal processor should still determine the average signal frequency and estimate the higher order statistics. The

system is operated with the energy detection accumulators set to integrate more than one signal burst, which forces the energy distribution signal processing technique to be used. In this mode, an average of n signal bursts would be measured. Averaging the signal bursts increases the measured signal-to-noise ratio at the expense of a random smearing of signal frequencies. The amount of frequency smearing is dependent on the data rate and turbulence bandwidth. This process improves the accuracy of the average measurement, but the measurement of standard deviation is at best only an estimate.

This technique may also be used in laminar flow applications where the increase in signal-to-noise ratio will allow a decrease in residual f'/F, and therefore increase measurement accuracy. The measurement of standard deviation is improved if the data rate is sufficiently high so that data averaging does not affect the frequency content of turbulence. If the data rate is low, the loss of accuracy due to the random integration times of the measurement will be greater than the increase in accuracy obtained by combining multiple measurements.

Simulation Testing of the Frequency Domain Laser Velocimeter Signal Processor

The operation of the control algorithms and the characteristics of the frequency domain laser velocimeter signal processor were tested by means of computer simulation of laser velocimeter signal bursts and by modeling of the signal processor. The simulation of the signal burst was by means of Poisson shot noise models generated in the manner described in reference 8. These models could be adjusted from the photon-resolved regime, through photon pileup, to photomultiplier saturation. The model of the signal processor includes ADC, AGC, and AFC circuitry; signal detection circuitry; digital filter banks; zero crossing detection circuitry; energy detection circuitry; and signal processing algorithms to be implemented in the controlling microprocessor firmware. A typical test consisted of generating a series of signal bursts with a selected average photon count, average signal visibility, average oscillation frequency, and standard deviation of oscillation frequency. The oscillation frequency for each signal burst was statistically selected based on Monte Carlo methods with a Gaussian probability distribution of signal frequencies based on the requested average and standard deviation. The theoretical signal burst is generated based on the selected oscillation frequency and input visibility function and used as the driver for generation of the signal burst based on the algorithm from reference 8 (fig. 2). This burst is then input to the model of the FDLVSP for setup and/or processing according to the procedure above (fig. 13). Once the setup phase is completed, 100 signal bursts are input to and processed by the FDLVSP. The statistics of the measured results are calculated and compared with the statistics of the input ensemble used to generate the signal bursts. This direct comparison of data removes the assumption that the characteristics of the 100 signal bursts agree with the requested average frequency and standard deviation. A model of a high-speed burst counter was developed to serve as a performance comparison. It used 4-pole Butterworth low- and high-pass filters, double threshold signal detection, zero crossing measurement by using a 500 MHz reference clock, and 5:8 count comparison error detection. Again the statistics of the input ensemble of signal bursts were compared to the output statistics of the measurement ensemble from the high-speed burst counter. It is noted that signal bursts that did not satisfy either the double threshold detection check and/or 5:8 error detection were not included in the measurement ensemble, whereas all measurements were included in the results from the FDLVSP.

The first series of comparison tests determined the measurement accuracy of f'/F for high-level signals (approximately 1500 photons per burst at a signal frequency of 25 MHz—example given in fig. 2(b)) from 0 to 20 percent. The results for a mean frequency F of 5.0 MHz are shown in figure 14. The measurement accuracies for both instrumentation techniques are approximately the same over the entire range of f'/F. The mean frequency was then increased to 25.0 MHz; the results are shown in figure 15. This test showed the effect of residual f'/F in the high-speed burst counter measurements below an f'/F of 1 percent, whereas the accuracy of the FDLVSP was unchanged. The increase of the mean frequency to 100.0 MHz (fig. 16) continued the trend with reduced counter accuracy over the entire range of f'/F, whereas again the FDLVSP results were unchanged. This effect may be seen directly in figure 17 where the data for the three center frequencies are overlaid for the high-speed burst counter in figure 17(a) and for the FDLVSP in figure 17(b).

The effect of signal-to-noise ratio on the measurements was tested by reducing the average photon count per signal burst from approximately 3000 per burst to approximately 150 per burst at a mean frequency of 25.0 MHz. As shown in figure 18, the high-speed burst counter has a residual f'/F approximately 2.5 times larger than the FDLVSP down to 300 photons per burst. As the input f'/F is increased from 0 to 1.0 percent (figs. 19 through 24), the

results from the FDLVSP match the input at an f'/F of 0.2 percent with bursts containing at least 900 photons. Signals with photon counts down to 500 match at 0.3 percent and signals down to 300 photons match at 0.4 percent. The high-speed burst counter results did not match until f'/F reached 1.0 percent and then had a great deal of scatter.

The effect of multiple bursts per measurement on the residual f'/F is illustrated in figure 25, where the average input signal burst contained 150 photons. As shown, adding the second signal burst reduced the residual f'/F from 1.0 percent to below 0.4 percent. The trend continued until the residual reached 0.2 percent at 6 bursts per measurement, which is the limit for the high signal-to-noise ratio conditions (fig. 18). Figure 26 is a repeat of figure 18 with the overlay of the results from the average of 5 bursts per measurement. These data show a reduction of 50 percent in residual f'/F up to signals containing 1100 photons per burst. Measurements could also be made from signal bursts with as few as 60 photons per burst. Therefore, decreases in residual f'/F may be obtained from signals with lower photon counts by the integration of energies from multiple signal bursts in the manner of the photon correlator.

Concluding Remarks

A frequency domain laser velocimeter signal processor (FDLVSP) has been described. It has been shown through simulations to provide the same or better accuracy as current laser velocimeter signal processing techniques without operator intervention. The new signal processor is a "smart" instrumentation system that determines its proper operating parameters from the signals themselves and reconfigures itself to optimize measurement accuracy. The system provides the same measurement capabilities as the high-speed burst counter in instantaneous measurements from single signal bursts, the same automatic gain control and automatic frequency control as the frequency tracker, and the same immunity to errors derived from signal-to-noise ratio as the photon correlator.

Simulation results have shown residual values of the turbulence intensity parameter f'/F to be 0.2 percent from signal bursts with as few as 600 photons, which represents a factor of 2.5 below the residual values obtained from the high-speed burst counter. Above this level of f'/F (actually above 1.0 percent when the high-speed burst counter becomes accurate), the FDLVSP has accuracies comparable to the high-speed burst counter up to an input f'/F of 20 percent without the subjective setting of bandpass filters as required by the counter. The simulation results show accurate measurements (residuals less than 1.0 percent) from signals with average photon counts down to 150 photons per burst. By averaging five signal bursts, measurements down to the photon resolved region of 60 photons per burst (an average of 3 photons per cycle for the 20-cycle burst) yielded residuals of less than 0.3 percent.

NASA Langley Research Center
Hampton, VA 23665-5225
July 21, 1987

References

1. Huffaker, Robert M.; Fuller, Charles E.; and Lawrence, T. R.: Application of Laser Doppler Velocity Instrumentation to the Measurement of Jet Turbulence. [Preprint] 690266, Soc. Automotive Engineers, Jan. 1969.
2. Fridman, J. D.; Kinnard, K. F.; and Meister, K.: Laser Doppler Instrumentation for the Measurement of Turbulence in Gas and Fluid Flows. *Proceedings of the Technical Program—Electro-Optical Systems Design Conference,* Karl A. Kopetzky, ed., Industrial and Scientific Conference Management, Inc., c.1970, pp. 128–146.
3. Iten, Paul D.; and Mastner, Jiri: Laser Doppler Velocimeter Offering High Spatial and Temporal Resolution. *Flow—Its Measurement and Control in Science and Industry,* Volume One, Part Two, R. E. Wendt, Jr., ed., Instrument Soc. of America, 1974, pp. 1007–1013.
4. Lennert, A. E.; Smith, F. H., Jr.; and Kalb, H. T.: Application of Dual Scatter, Laser, Doppler Velocimeters for Wind Tunnel Measurements. *International Congress on Instrumentation in Aerospace Simulation Facilities—ICIASF '71 Record,* IEEE Publ. 71-C-33 AES, Inst. of Electrical and Electronic Engineers, Inc., c.1971, pp. 157–167.
5. Asher, J. A.: LDV Systems Development and Testing. *The Use of the Laser Doppler Velocimeter for Flow Measurements,* W. H. Stevenson and H. D. Thompson, eds., Contract N00014-67-A0226-005, Purdue Univ., Nov. 1972, pp. 338–347. (Available from DTIC as AD 753 243.)
6. Pike, E. R.: The Application of Photon-Correlation Spectroscopy to Laser Doppler Velocimetry. *The Use of the Laser Doppler Velocimeter for Flow Measurements,* W. H. Stevenson and H. D. Thompson, eds., Contract N00014-67-A0226-005, Purdue Univ., Nov. 1972, pp. 133–143. (Available from DTIC as AD 753 243.)
7. Griskey, R. G.; Balmer, R. T.; and Brinkley, J. L.: An Automatic Scanning LDV System. *Minnesota Symposium on Laser Anemometry—Proceedings,* E. R. G. Eckert, ed., Univ. of Minnesota, Jan. 1976, pp. 217–230.
8. Mayo, W. T., Jr.: Modeling Laser Velocimeter Signals as Triply Stochastic Poisson Processes. *Minnesota Symposium on Laser Anemometry—Proceedings,* E. R. G. Eckert, ed., Univ. of Minnesota, Jan. 1976, pp. 455–484.
9. Mayo, W. T., Jr.; Shay, M. T.; and Riter, S.: *The Development of New Digital Data Processing Techniques for Turbulence Measurements With a Laser Velocimeter.* AEDC-TR-74-53, U.S. Air Force, Aug. 1974. (Available from DTIC as AD 784 891.)

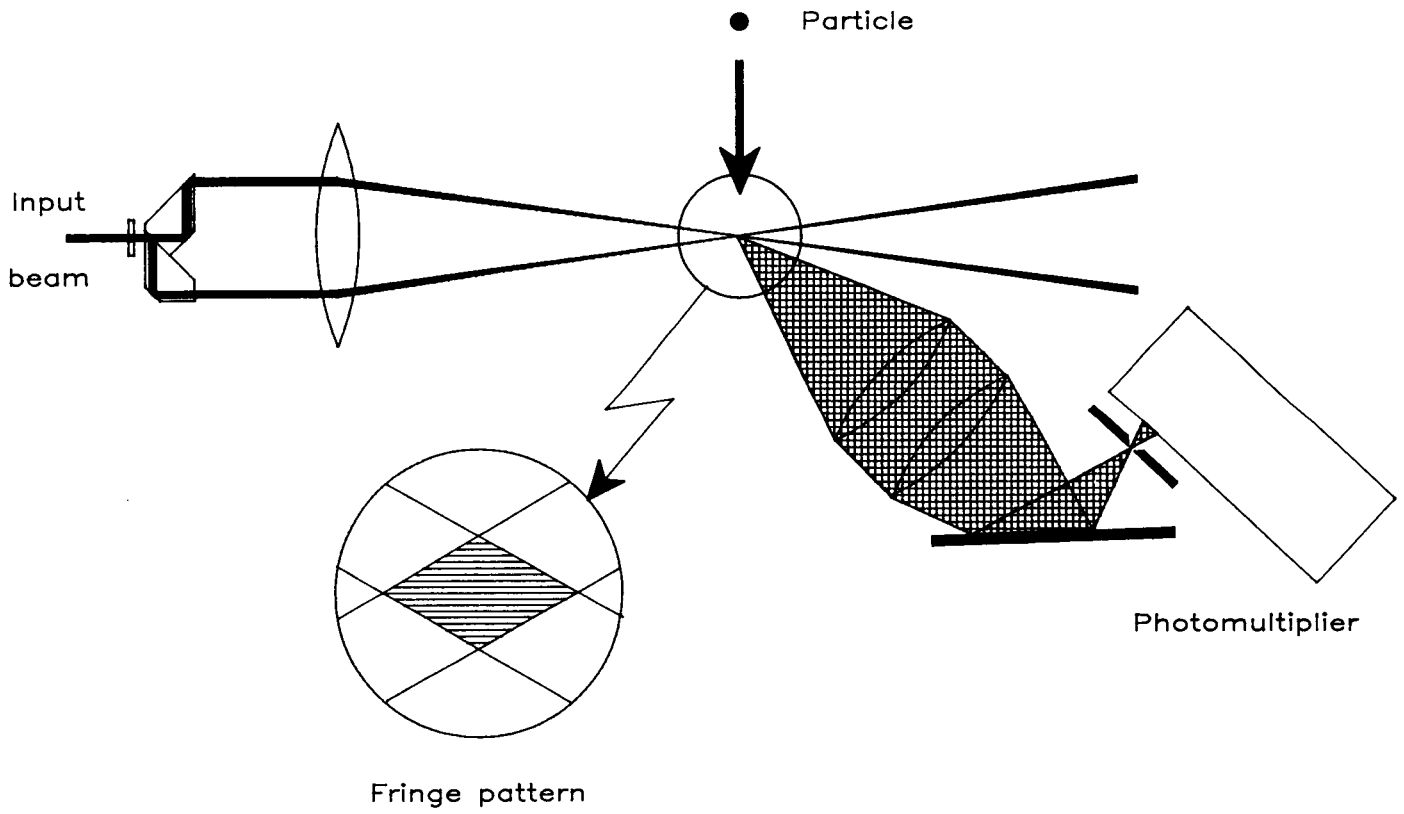

Figure 1. Schematic of single component, fringe-type laser velocimeter.

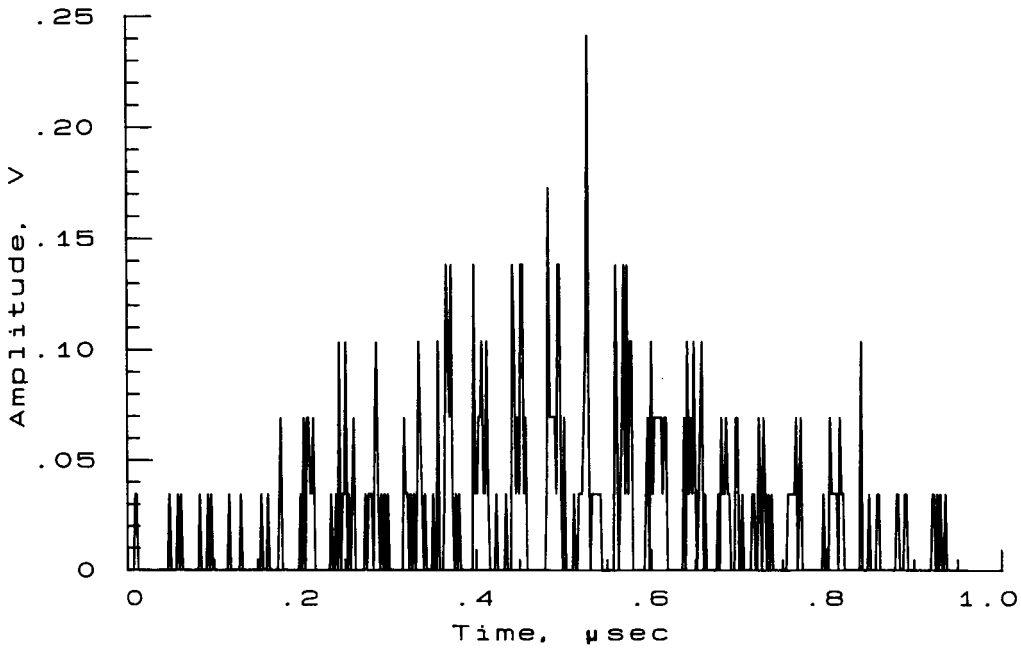

(a) Signal burst containing 310 photons.

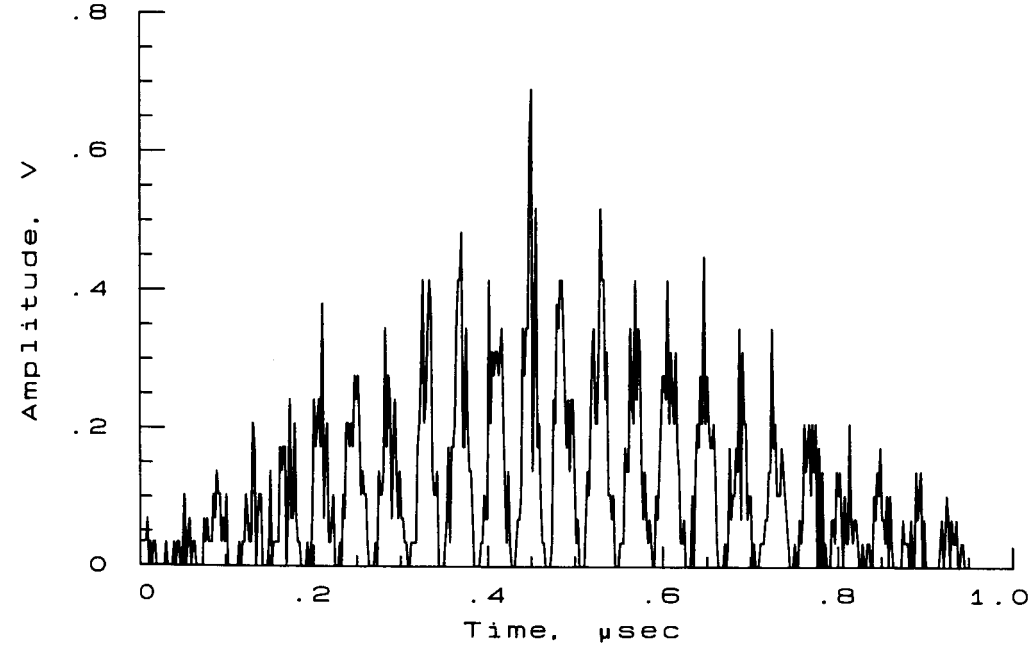

(b) Signal burst containing 1500 photons.

Figure 2. Signal burst from fringe-type laser velocimeter with modulation frequency of 25.0 MHz.

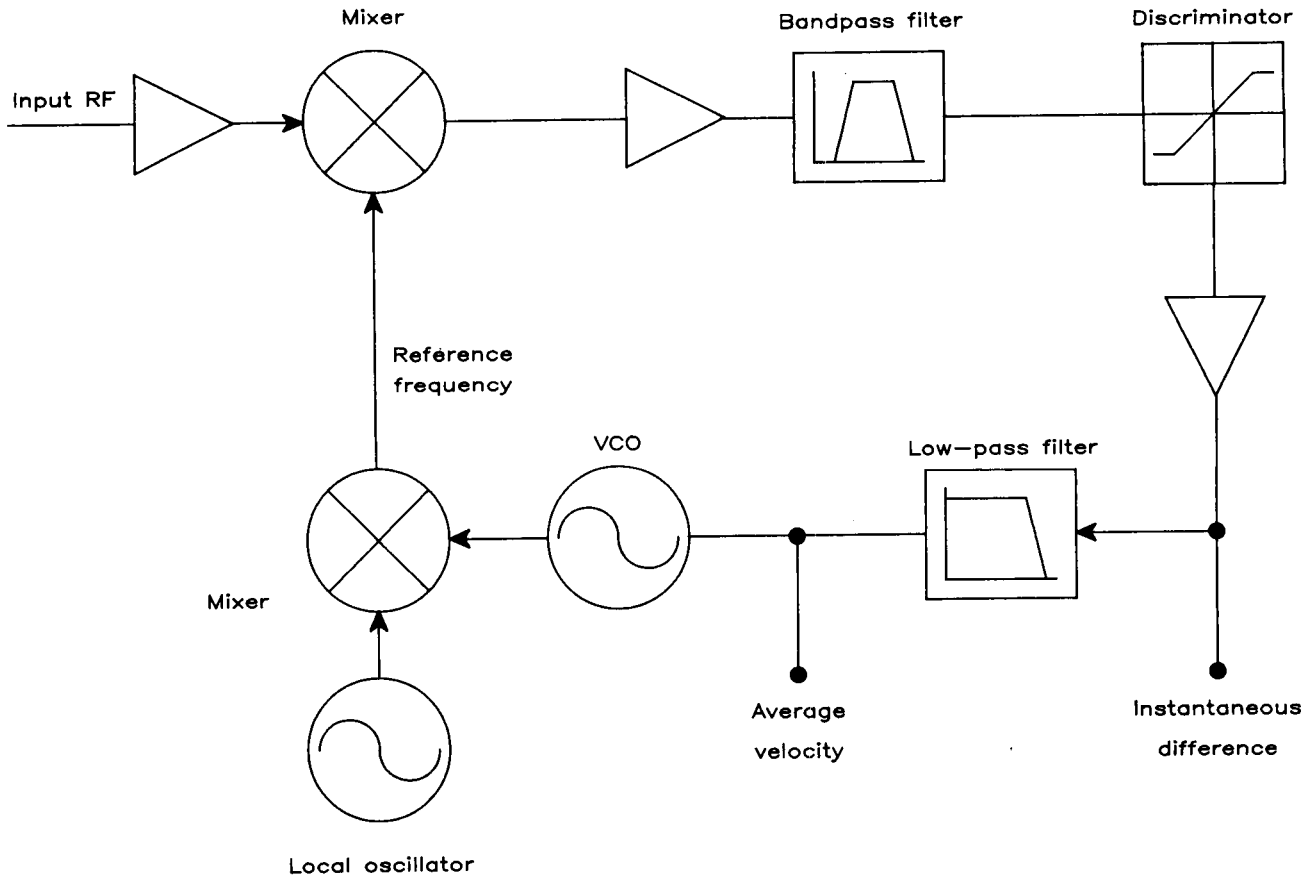

Figure 3. Schematic diagram of laser velocimeter wideband frequency tracker signal processor.

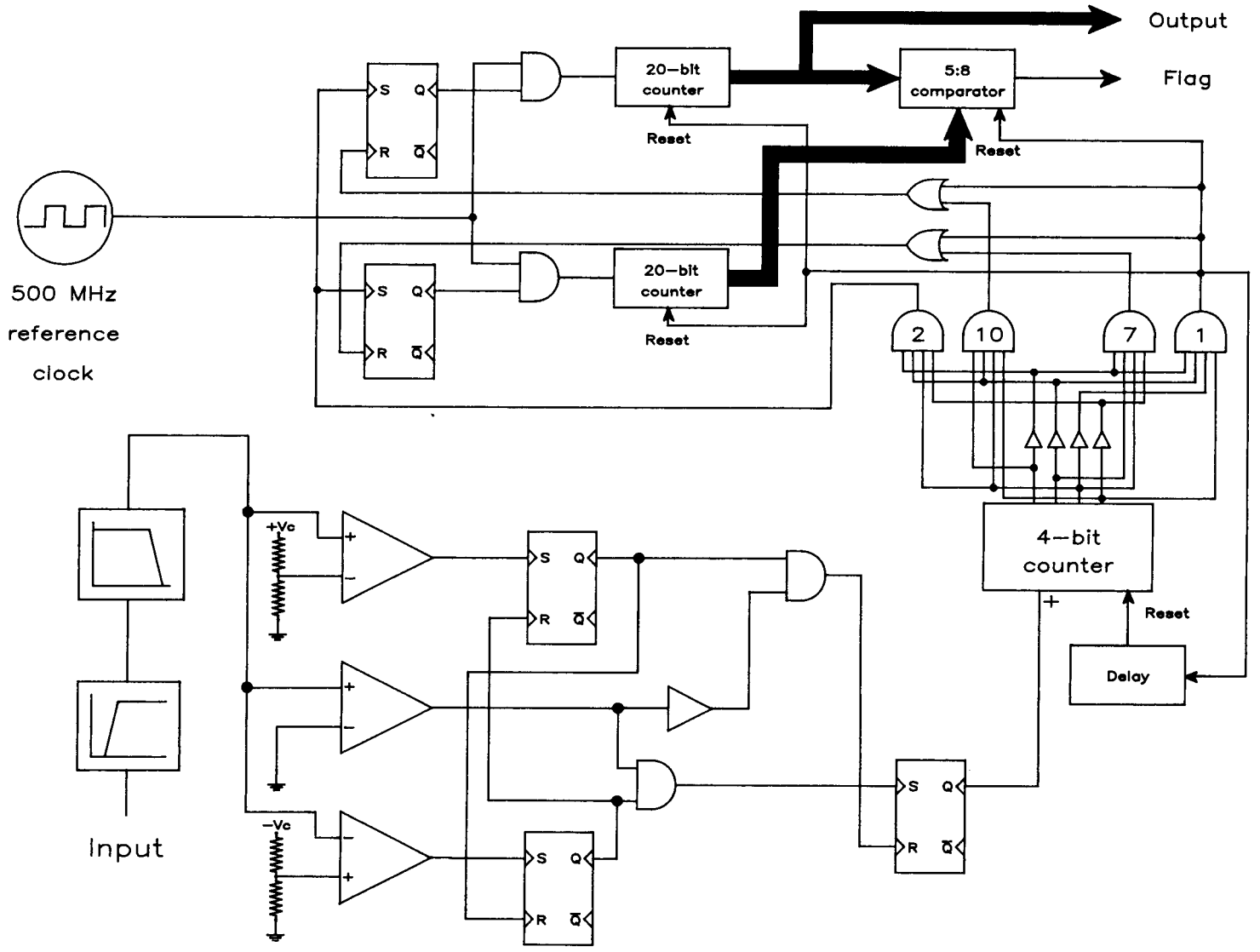

Figure 4. Schematic diagram of laser velocimeter high-speed burst counter signal processor.

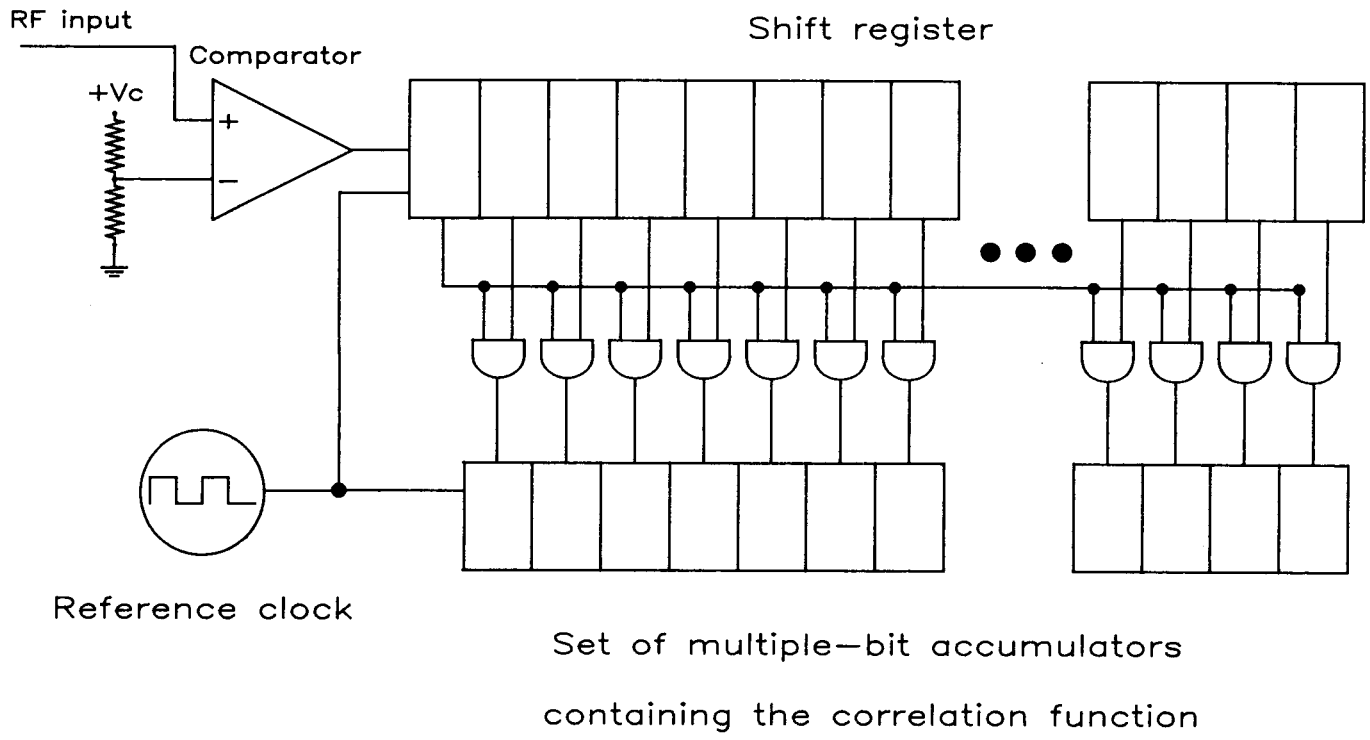

Figure 5. Schematic diagram of laser velocimeter single-bit photon correlator signal processor.

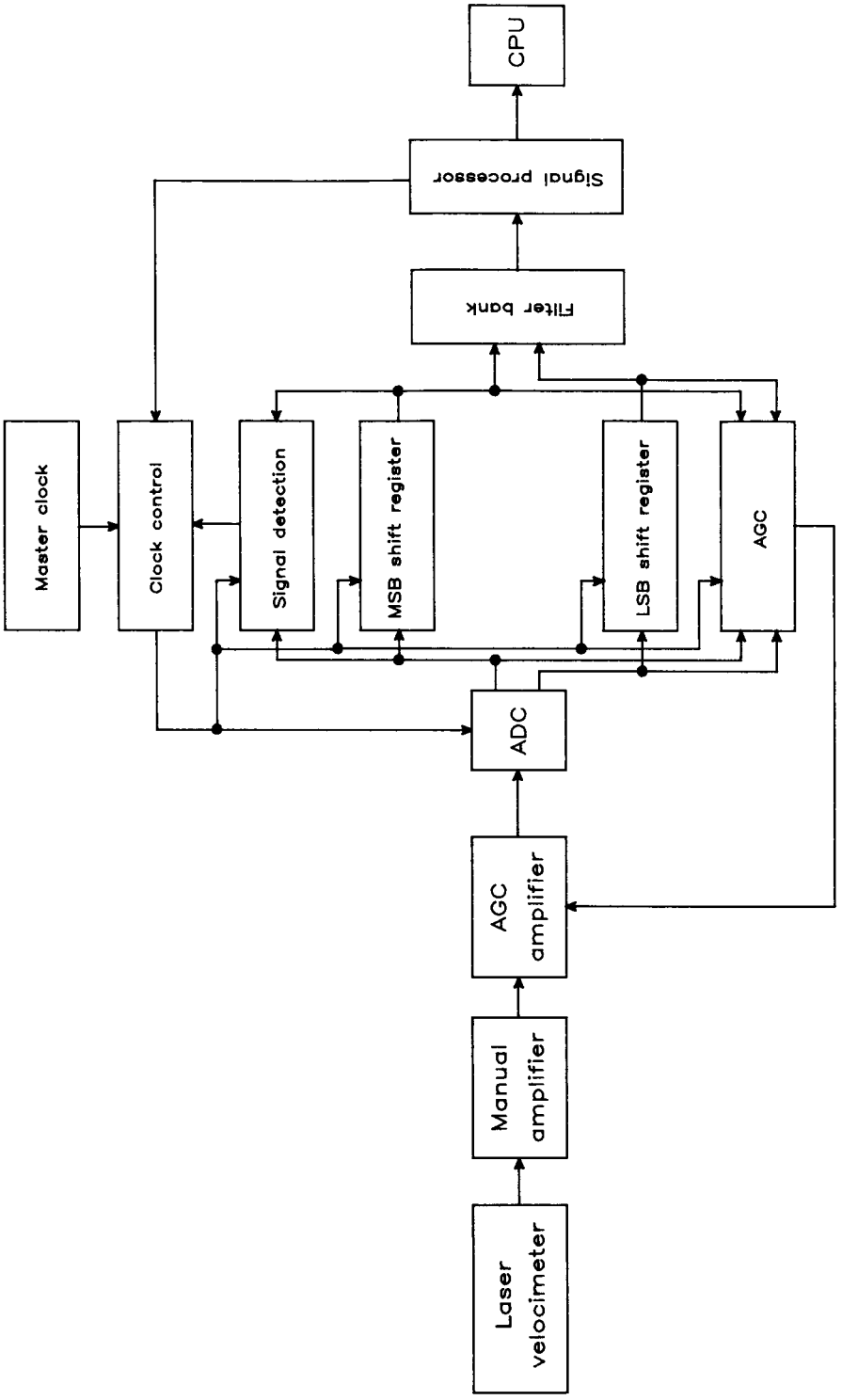

Figure 6. Block diagram of proposed frequency domain laser velocimeter signal processor.

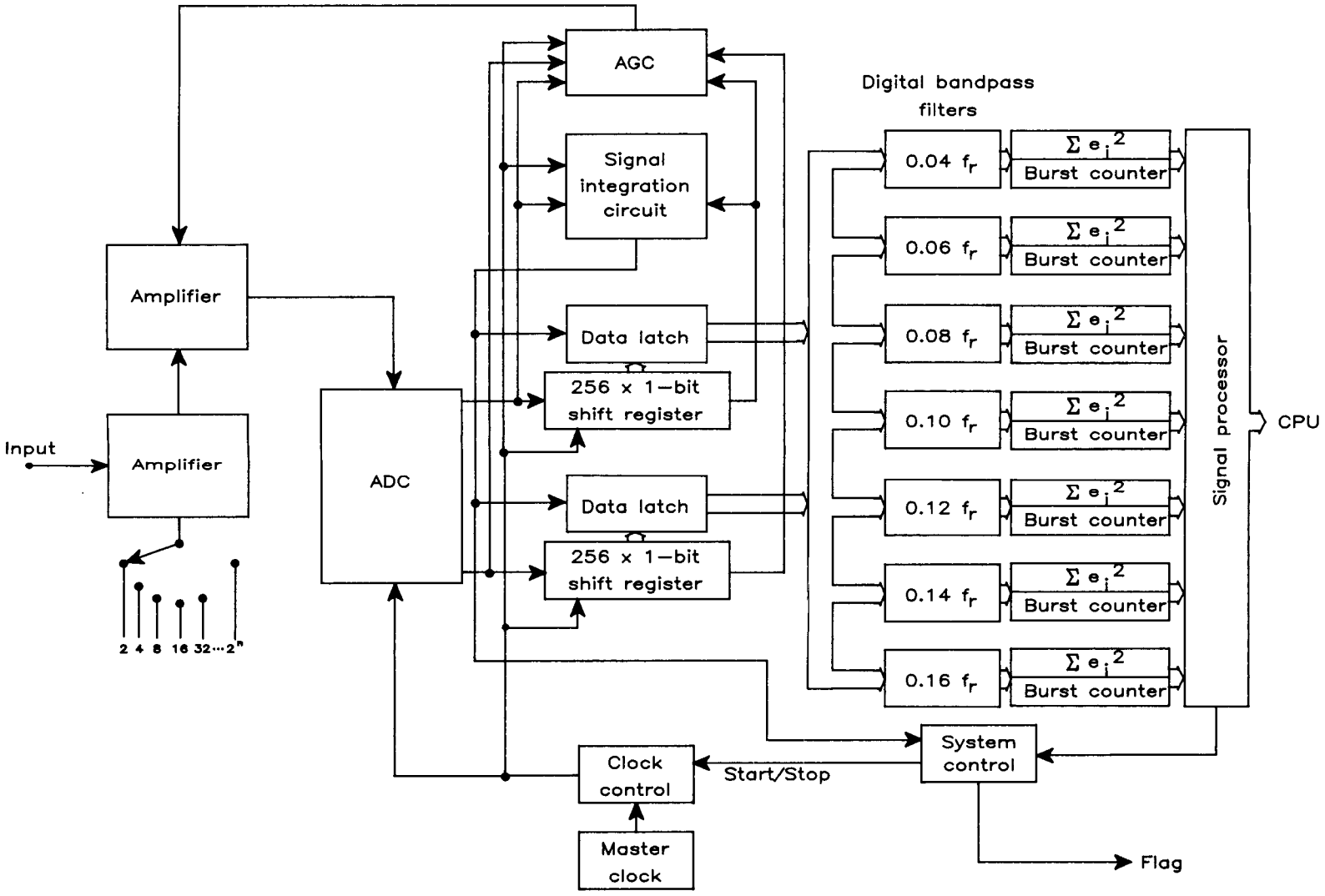

Figure 7. Schematic diagram of proposed frequency domain laser velocimeter signal processor.

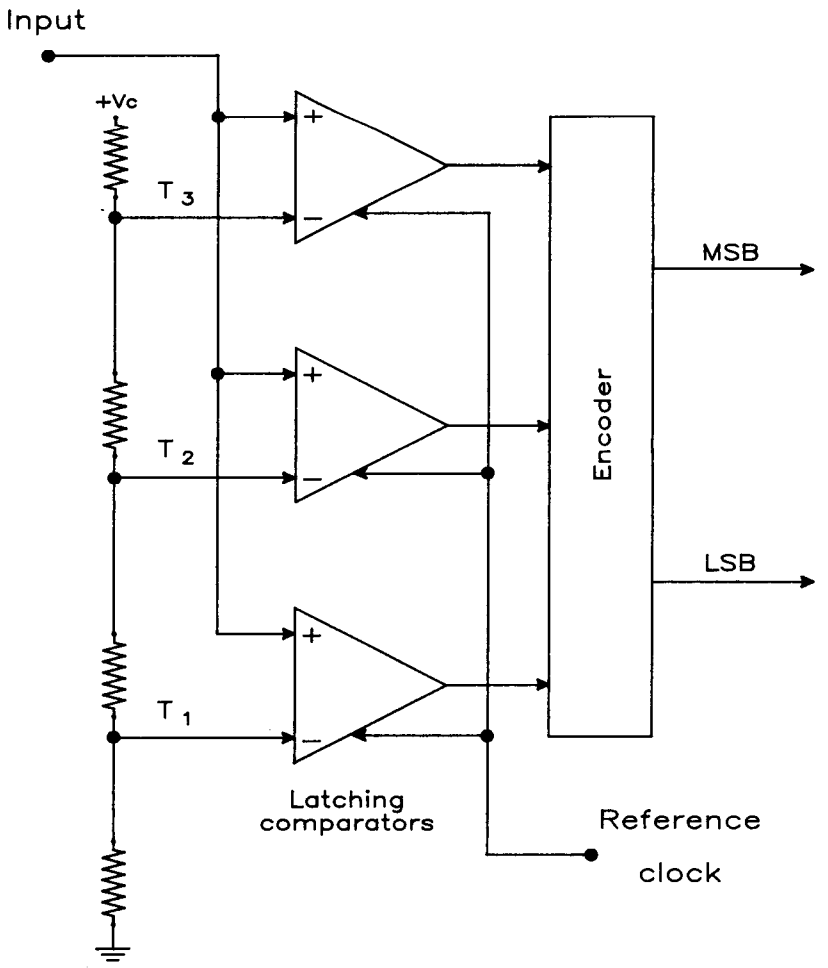

Figure 8. Schematic diagram of 2-bit analog-to-digital converter; T_1, T_2, and T_3 are chosen voltage thresholds.

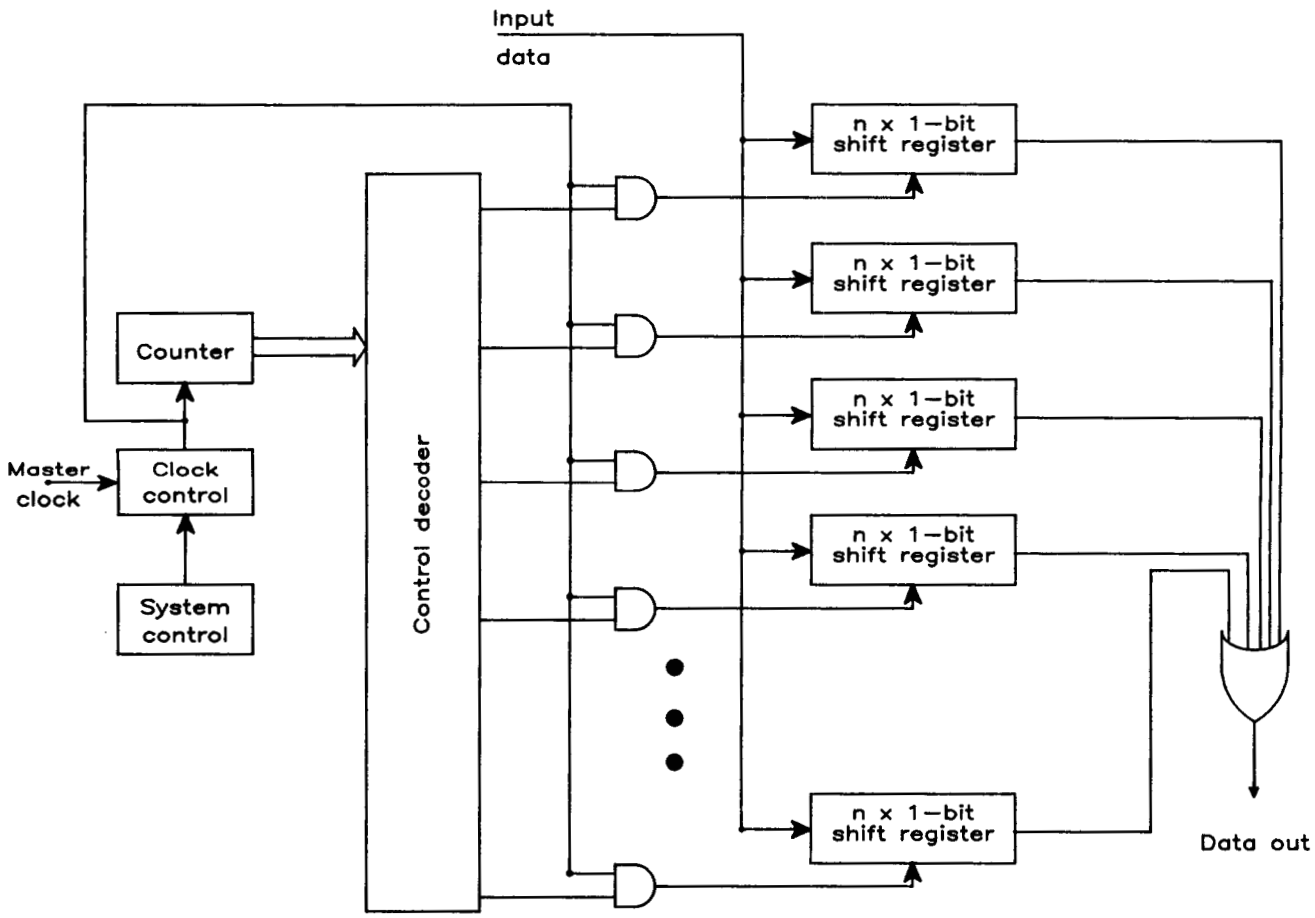

Figure 9. Schematic diagram of shift register circuits in parallel configuration.

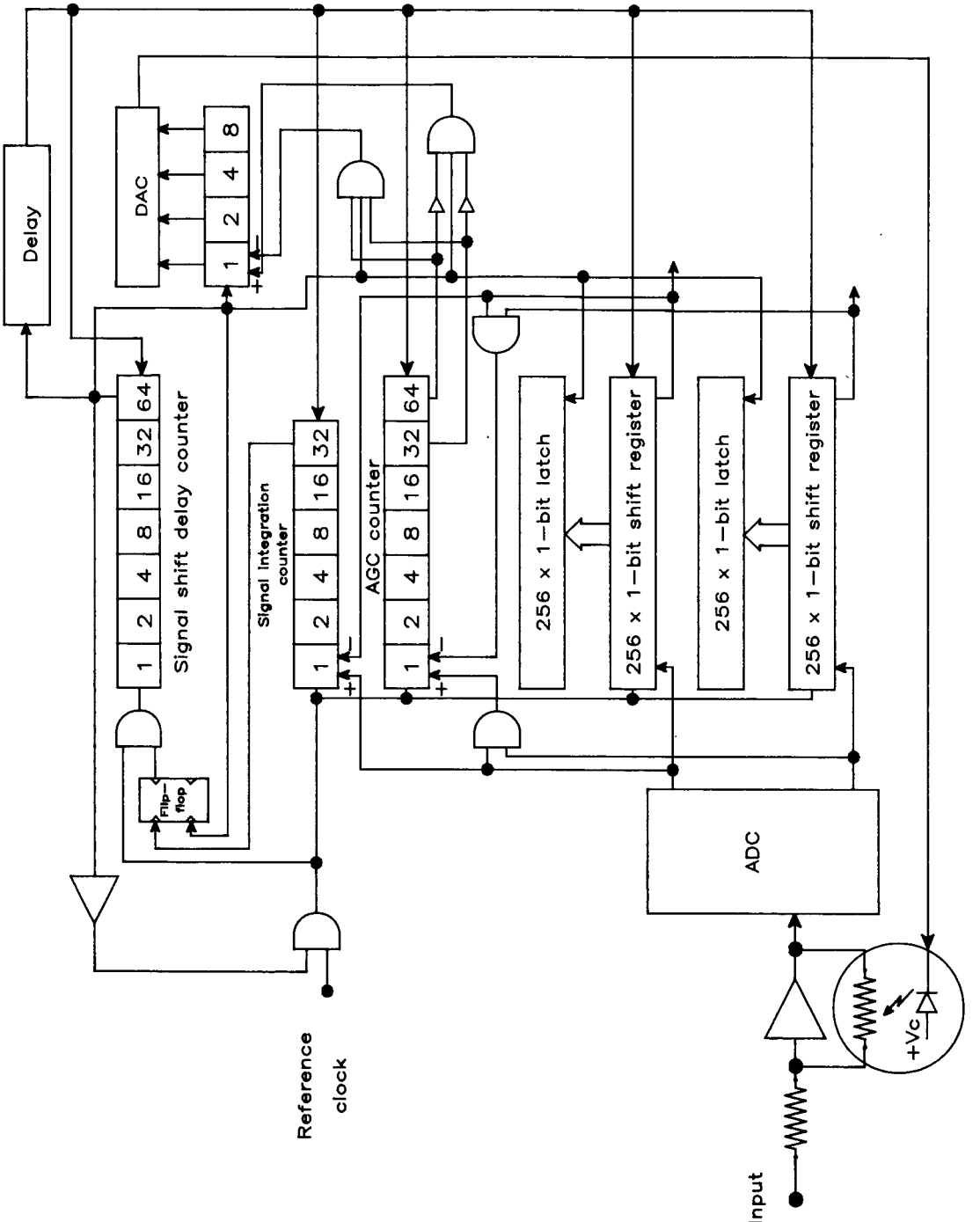

Figure 10. Schematic diagram of signal integration circuit and automatic gain circuitry.

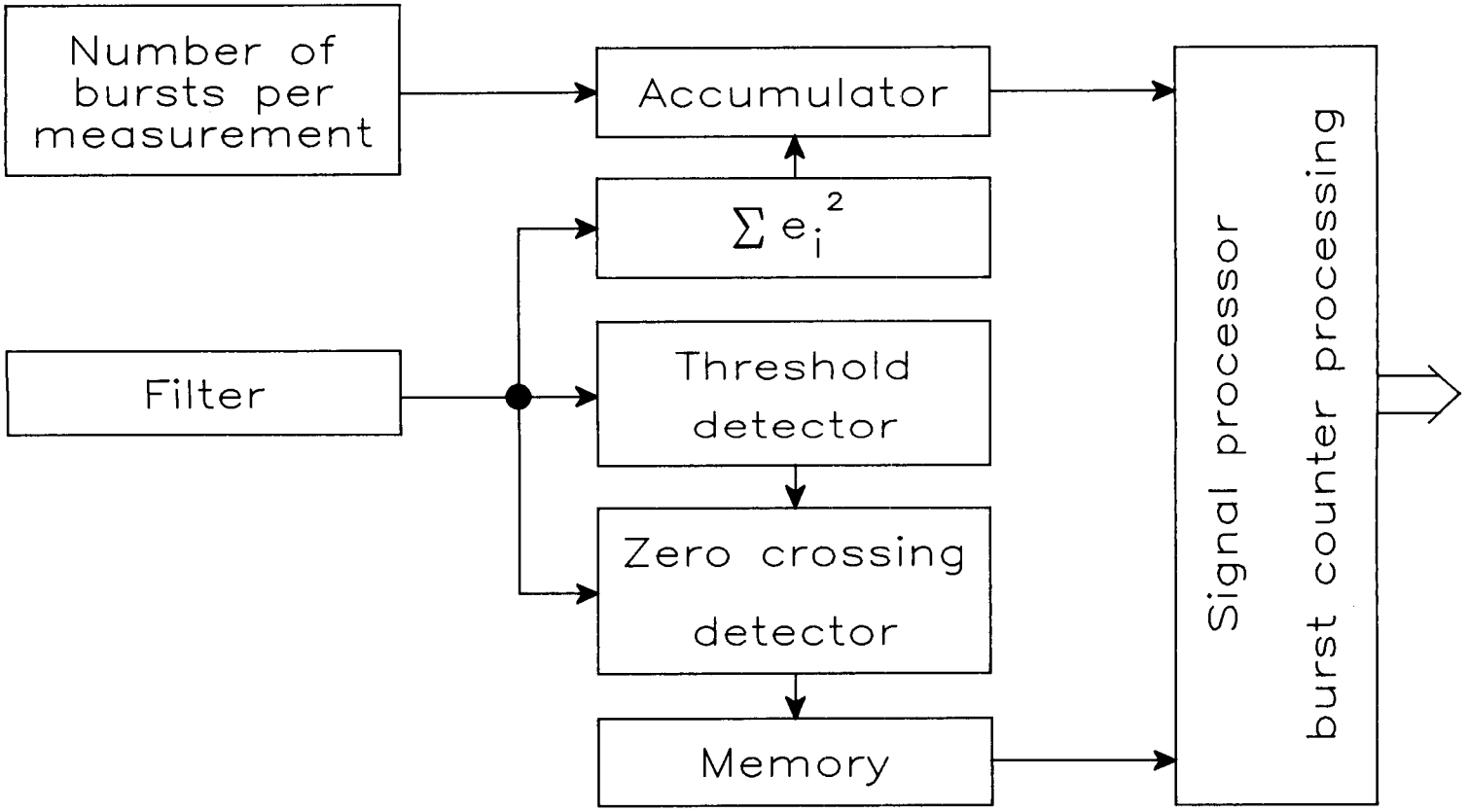

Figure 11. Schematic diagram of signal processing scheme.

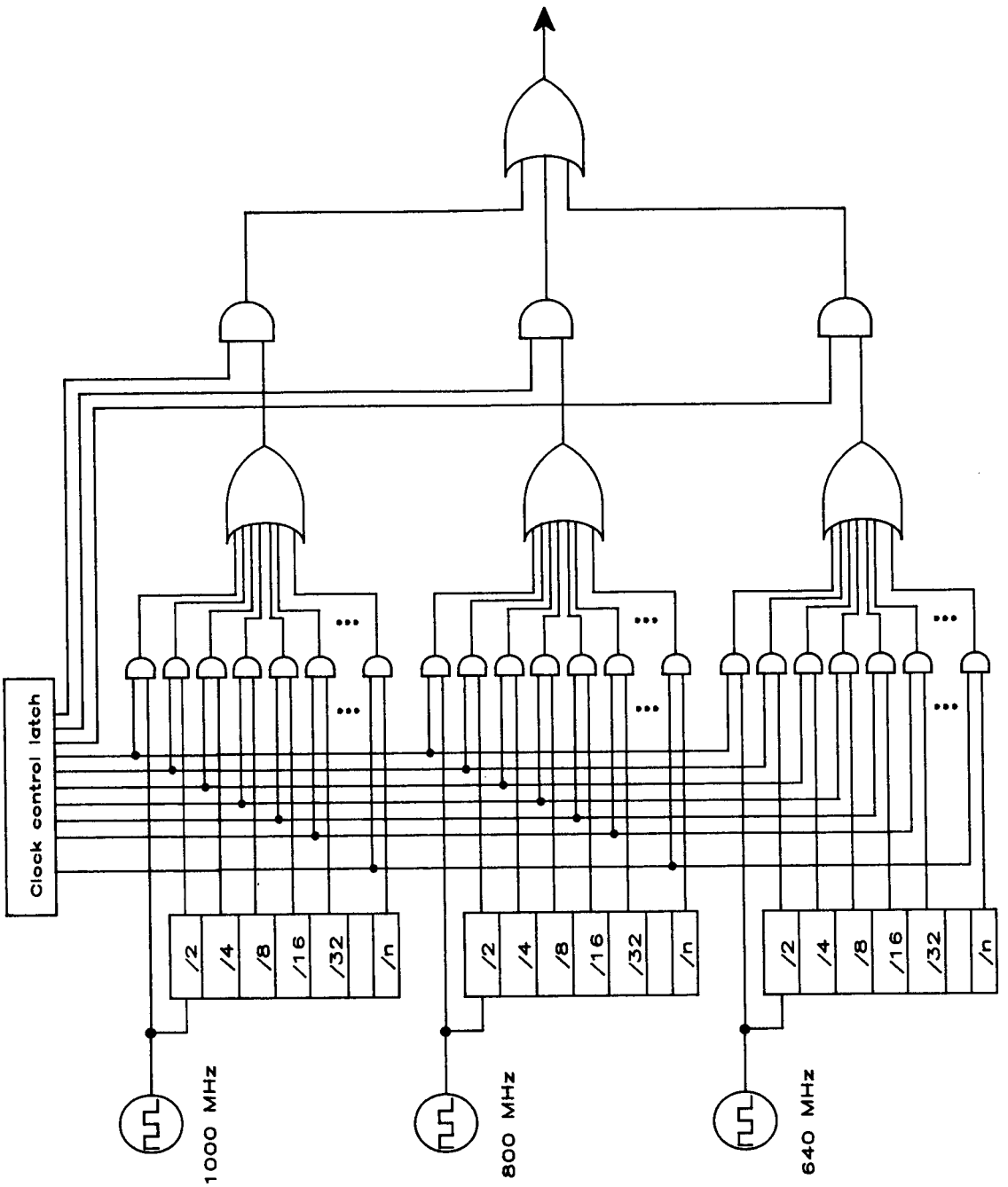

Figure 12. Schematic diagram of reference clock circuit.

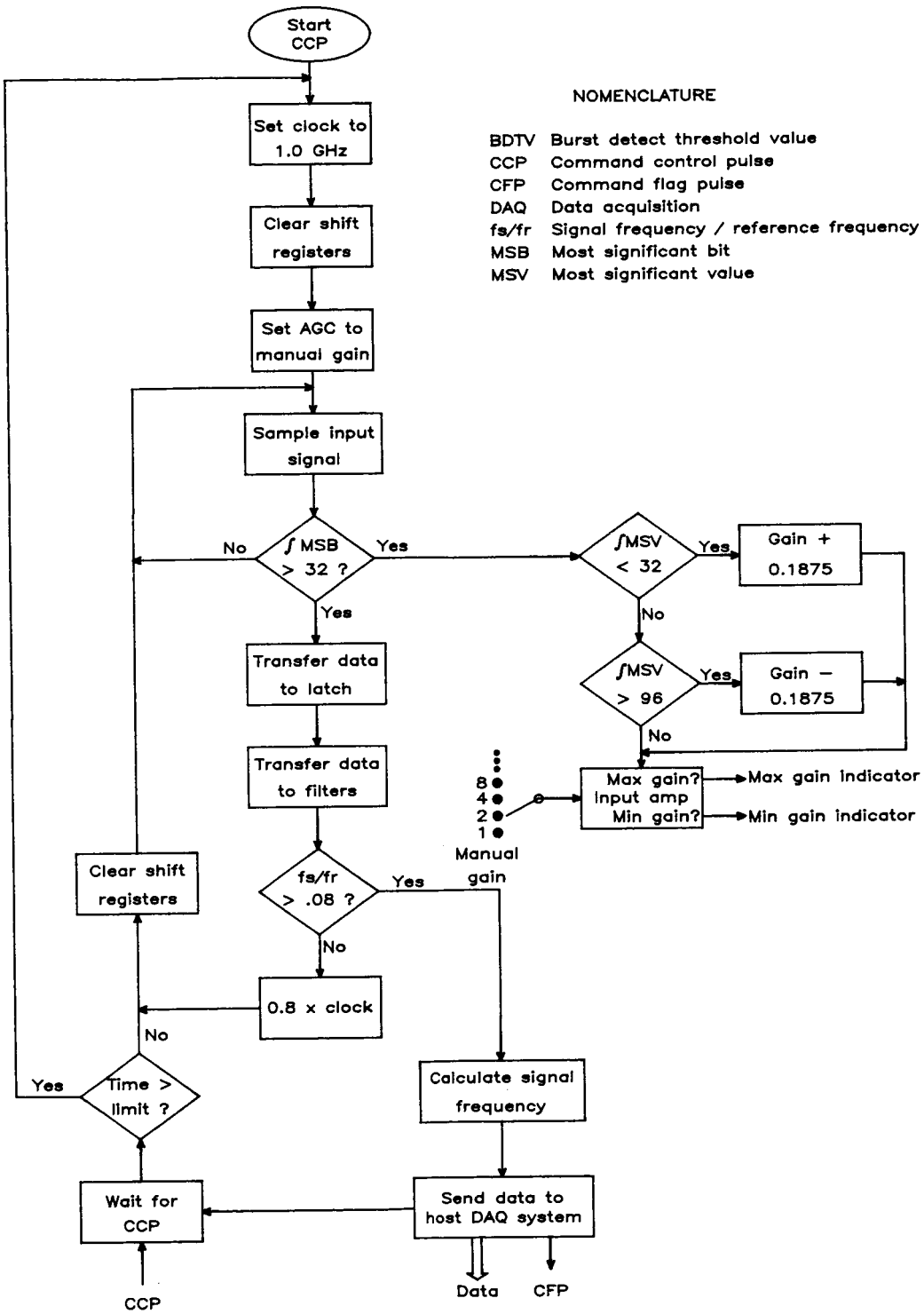

Figure 13. Logic flow diagram of setup phase of proposed frequency domain laser velocimeter signal processor.

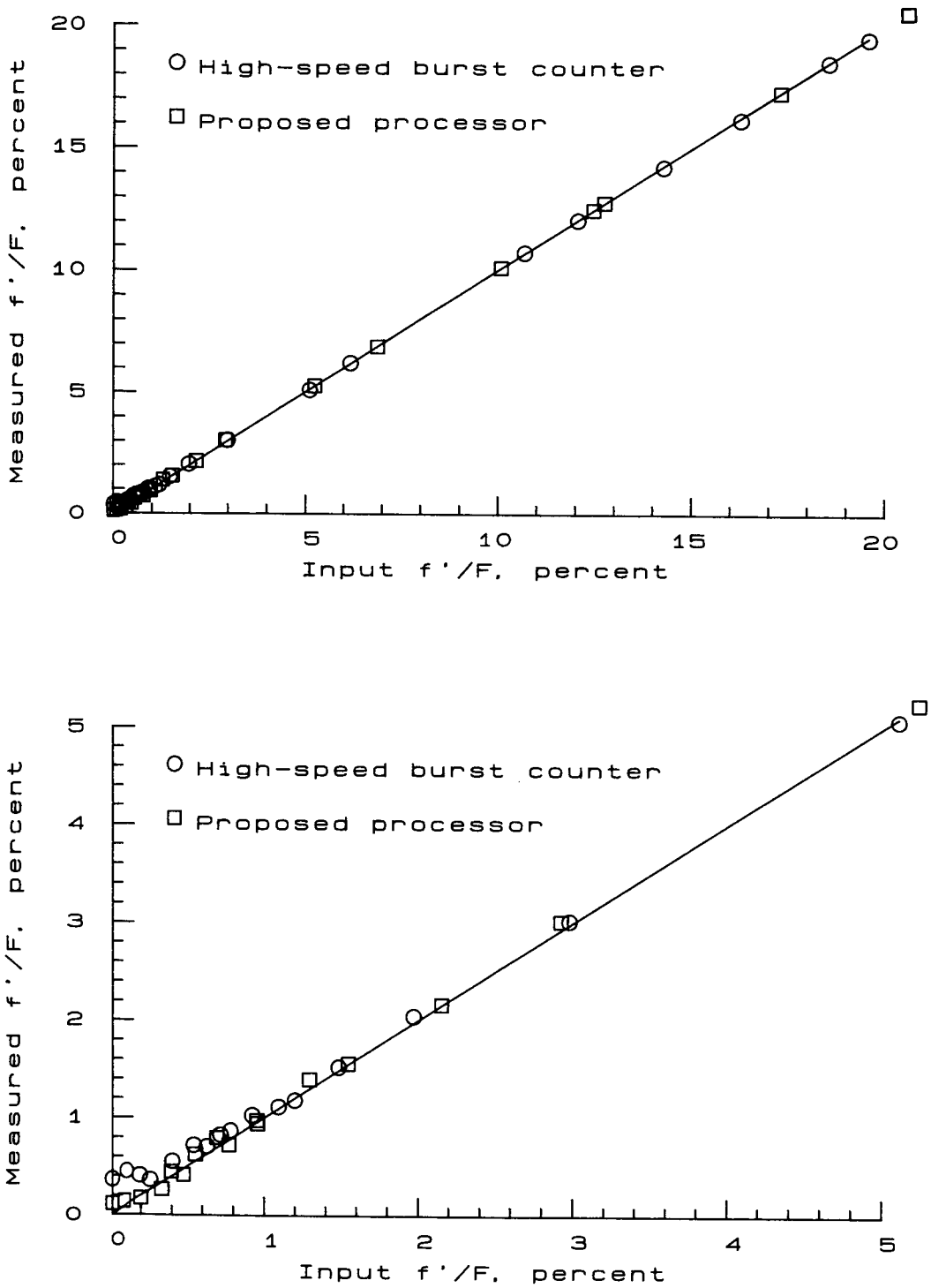

Figure 14. Simulation comparisons of input f'/F to measured f'/F for high-speed burst counter and frequency domain signal processor. Signal bursts have mean oscillation frequency of 5.0 MHz.

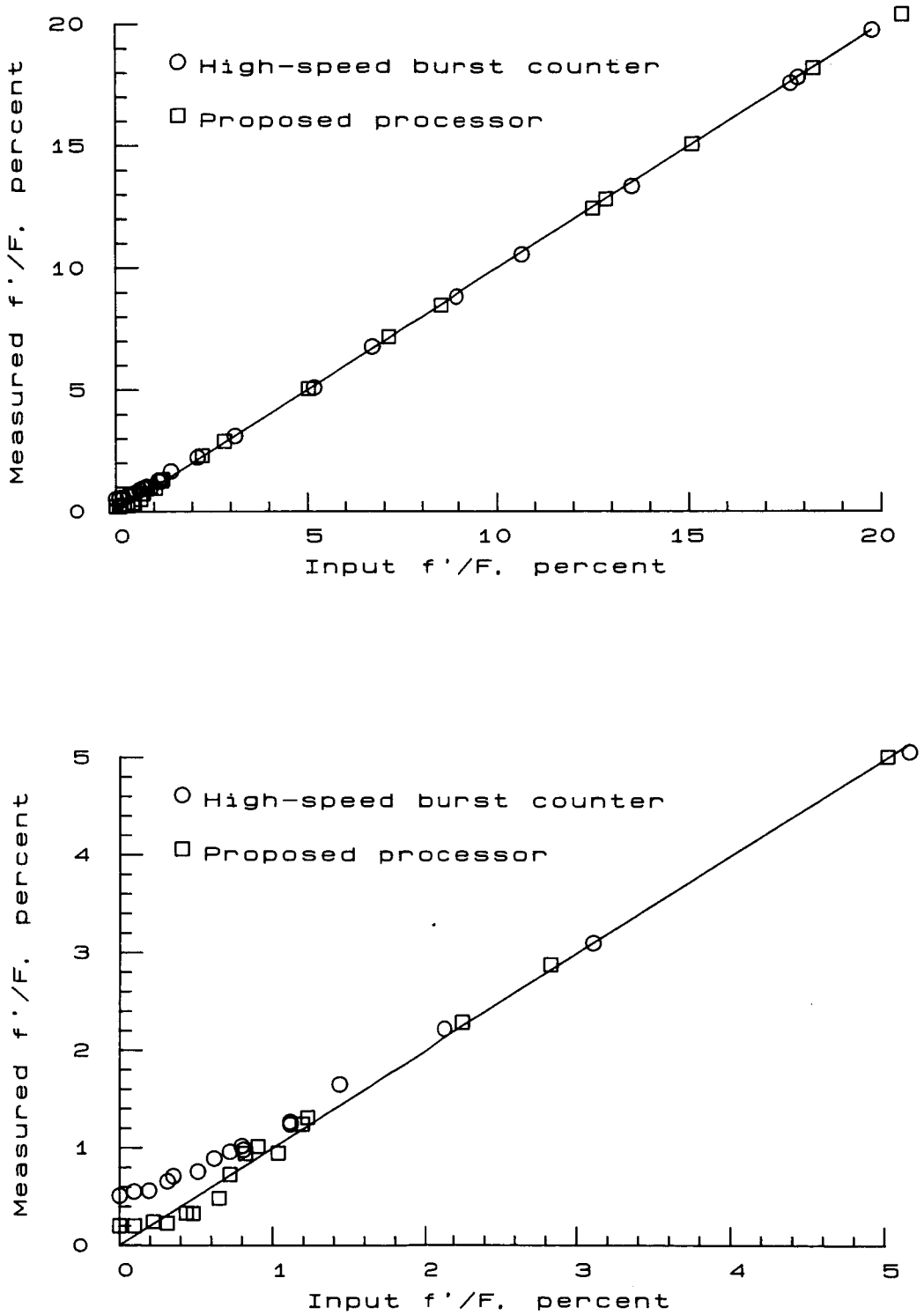

Figure 15. Simulation comparisons of input f'/F to measured f'/F for high-speed burst counter and frequency domain signal processor. Signal bursts have mean oscillation frequency of 25.0 MHz.

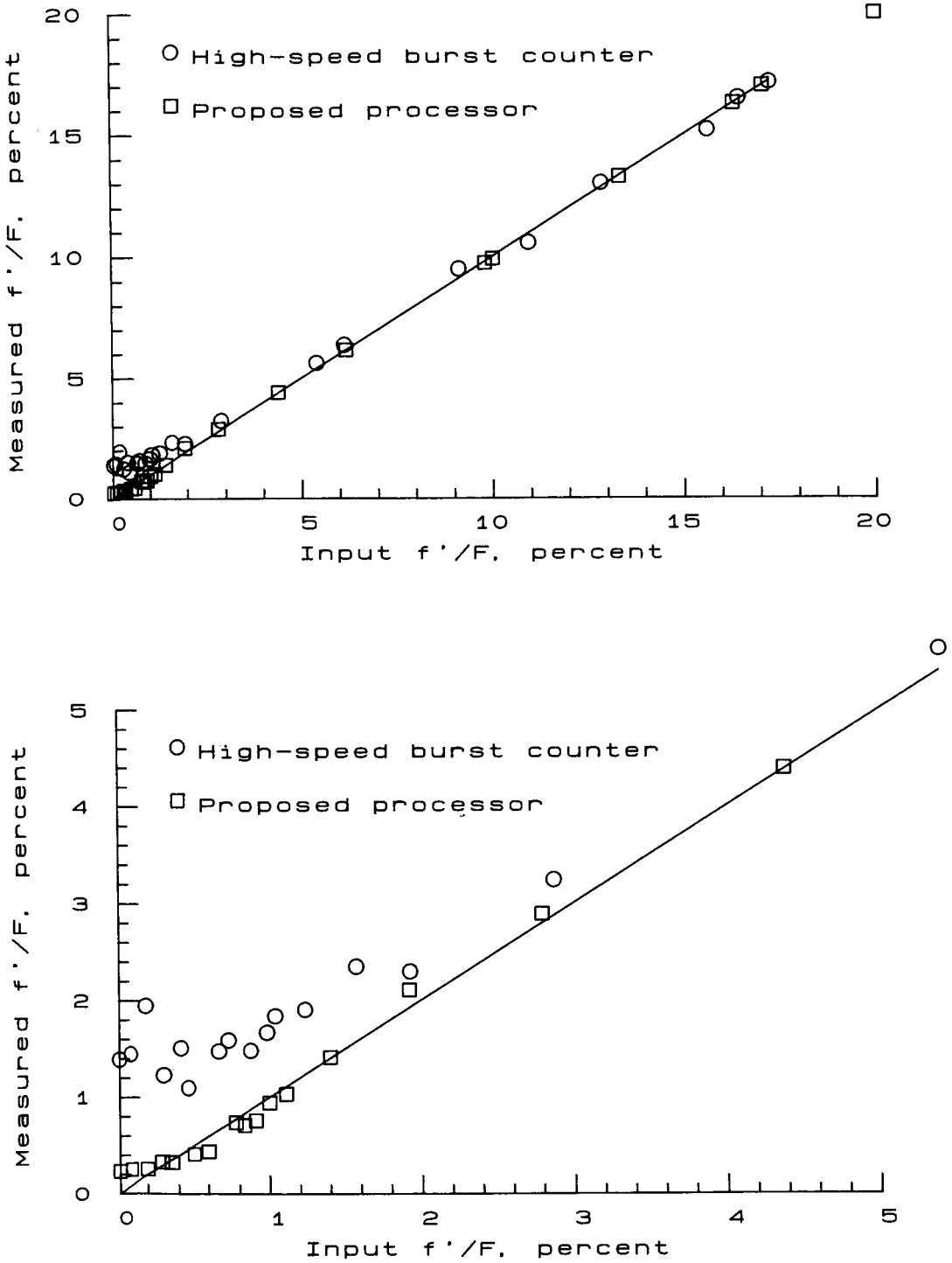

Figure 16. Simulation comparisons of input f'/F to measured f'/F for high-speed burst counter and frequency domain signal processor. Signal bursts have mean oscillation frequency of 100.0 MHz.

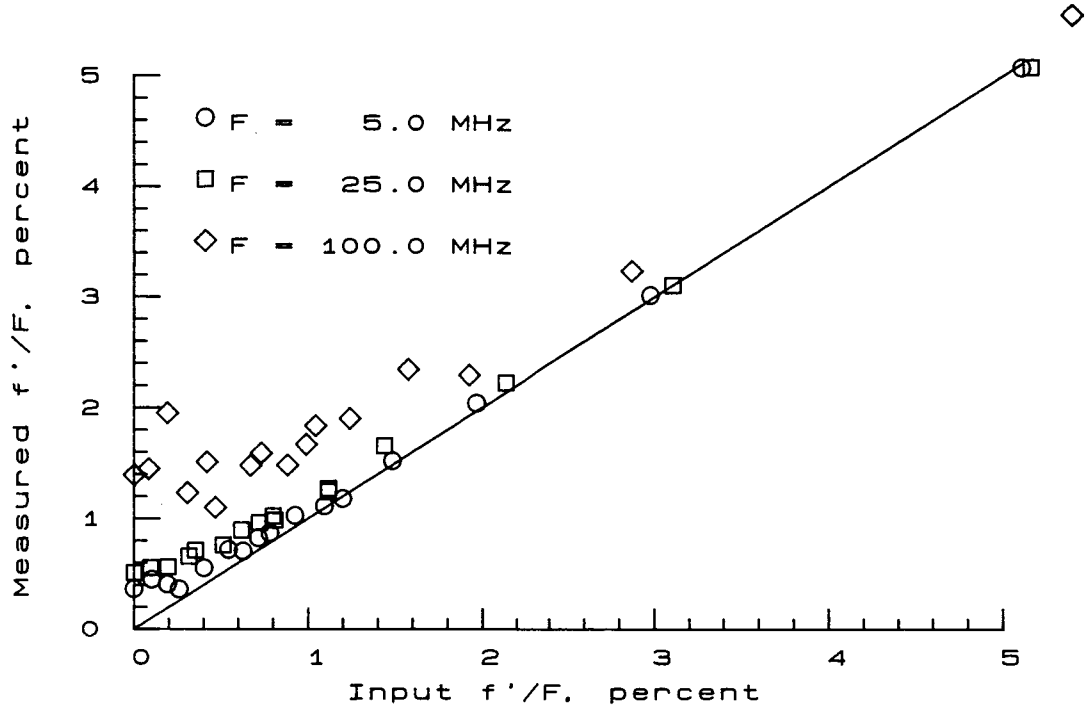

Figure 17(a). Simulation comparisons of input f'/F to measured f'/F for high-speed burst counter with mean oscillation frequencies of 5.0 MHz, 25.0 MHz, and 100.0 MHz.

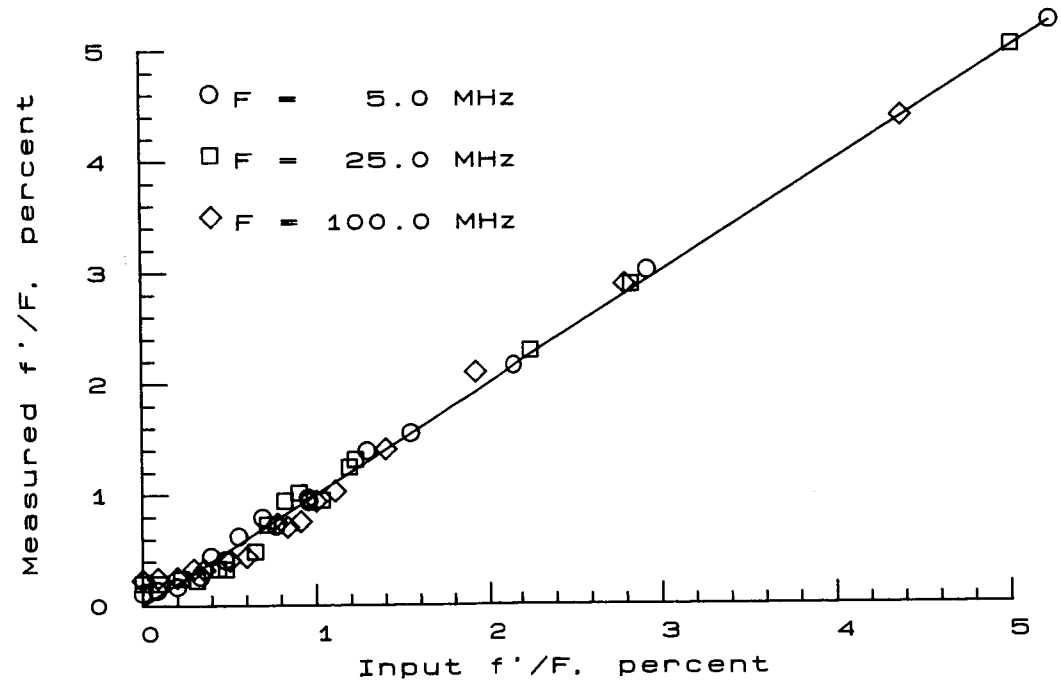

Figure 17(b). Simulation comparisons of input f'/F to measured f'/F for frequency domain signal processor with mean oscillation frequencies of 5.0 MHz, 25.0 MHz, and 100.0 MHz.

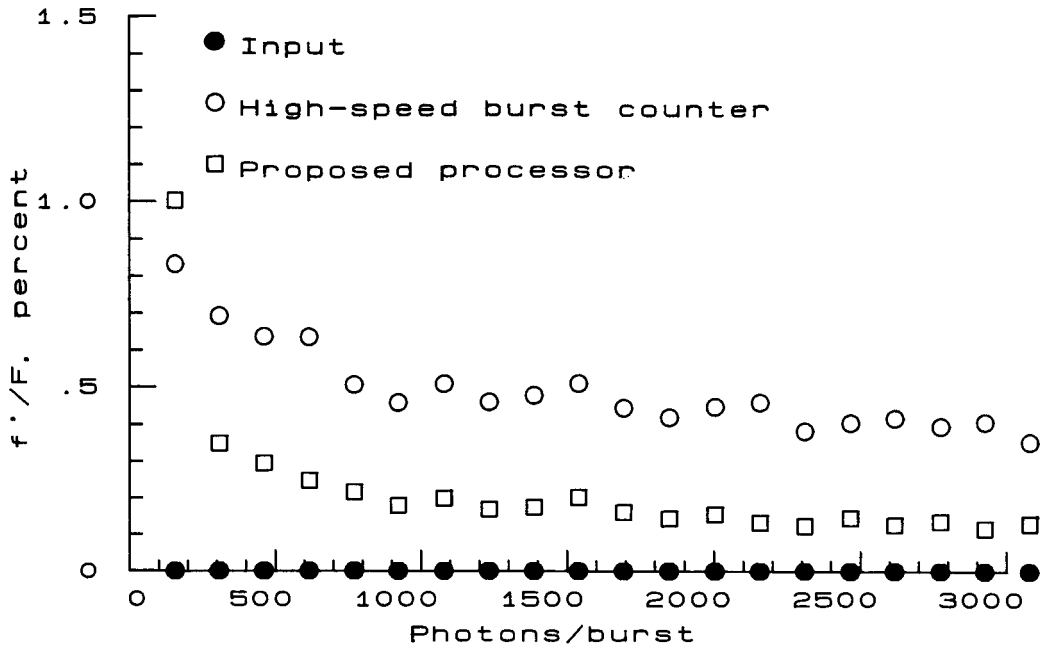

Figure 18. Simulation comparisons of input $f'/F = 0$ to measured f'/F for high-speed burst counter and frequency domain signal processor as a function of signal-to-noise ratio (photons/burst) at mean oscillation frequency of 25.0 MHz.

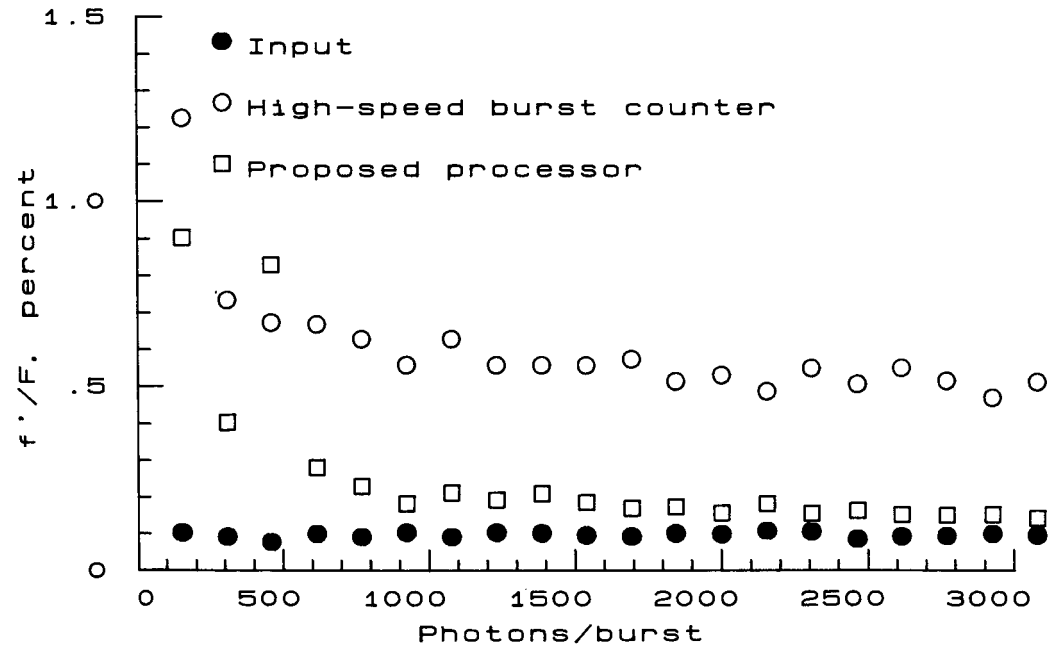

Figure 19. Simulation comparisons of input $f'/F = 0.1$ to measured f'/F for high-speed burst counter and frequency domain signal processor as a function of signal-to-noise ratio (photons/burst) at mean oscillation frequency of 25.0 MHz.

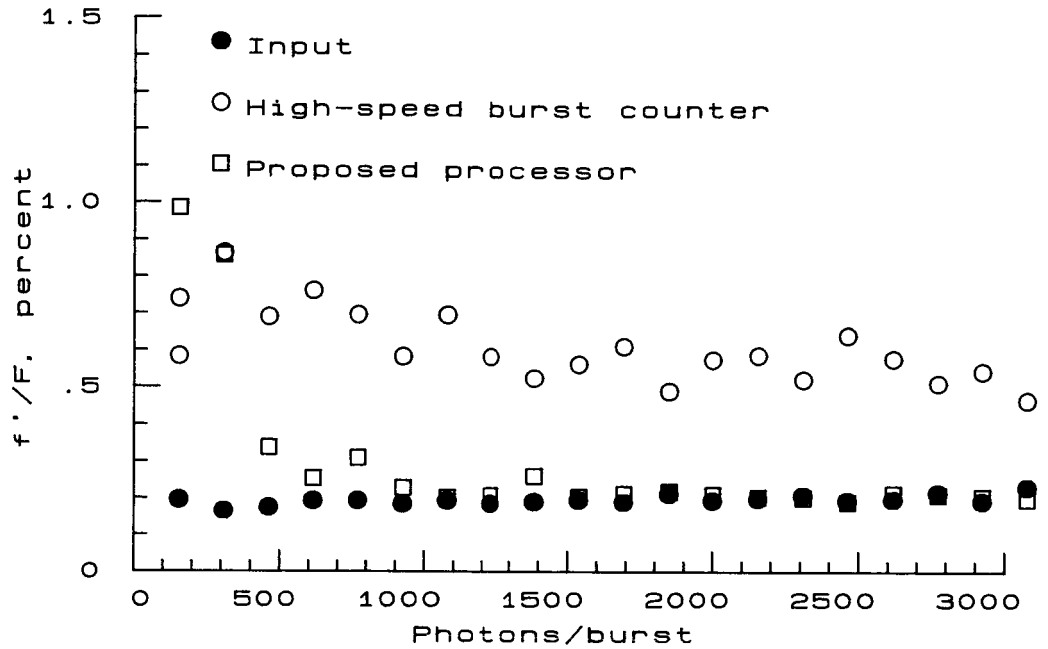

Figure 20. Simulation comparisons of input $f'/F = 0.2$ to measured f'/F for high-speed burst counter and frequency domain signal processor as a function of signal-to-noise ratio (photons/burst) at mean oscillation frequency of 25.0 MHz.

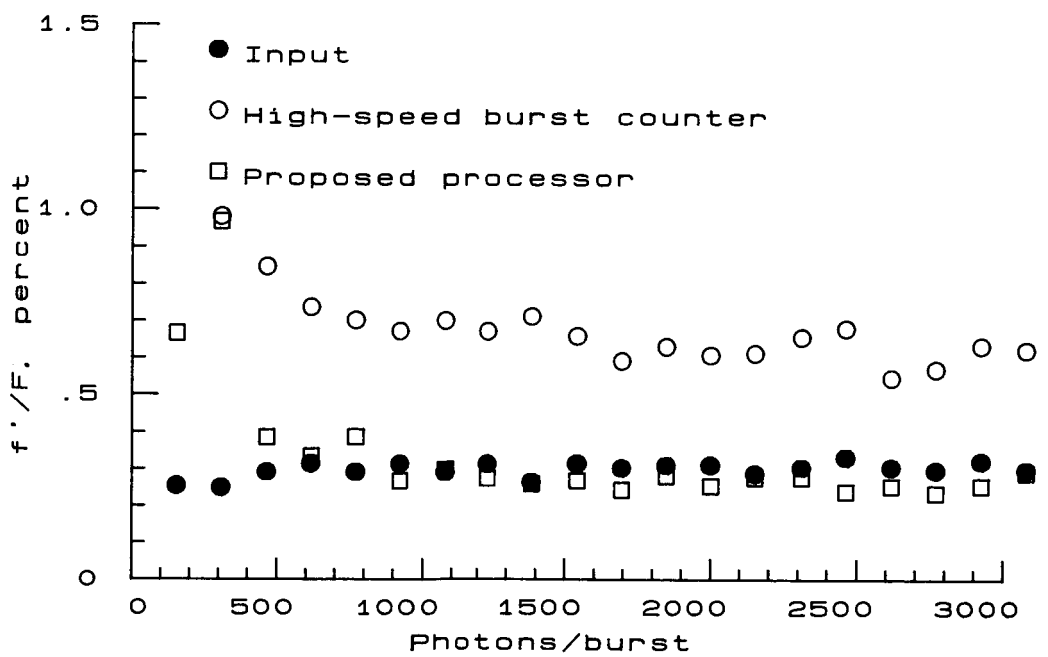

Figure 21. Simulation comparisons of input $f'/F = 0.3$ to measured f'/F for high-speed burst counter and frequency domain signal processor as a function of signal-to-noise ratio (photons/burst) at mean oscillation frequency of 25.0 MHz.

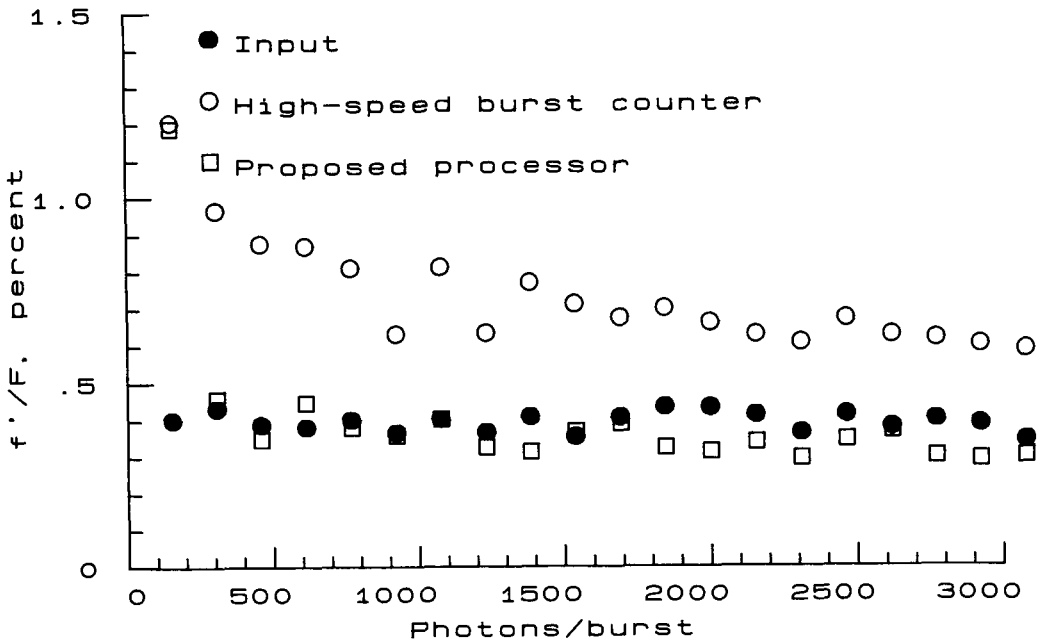

Figure 22. Simulation comparisons of input $f'/F = 0.4$ to measured f'/F for high-speed burst counter and frequency domain signal processor as a function of signal-to-noise ratio (photons/burst) at mean oscillation frequency of 25.0 MHz.

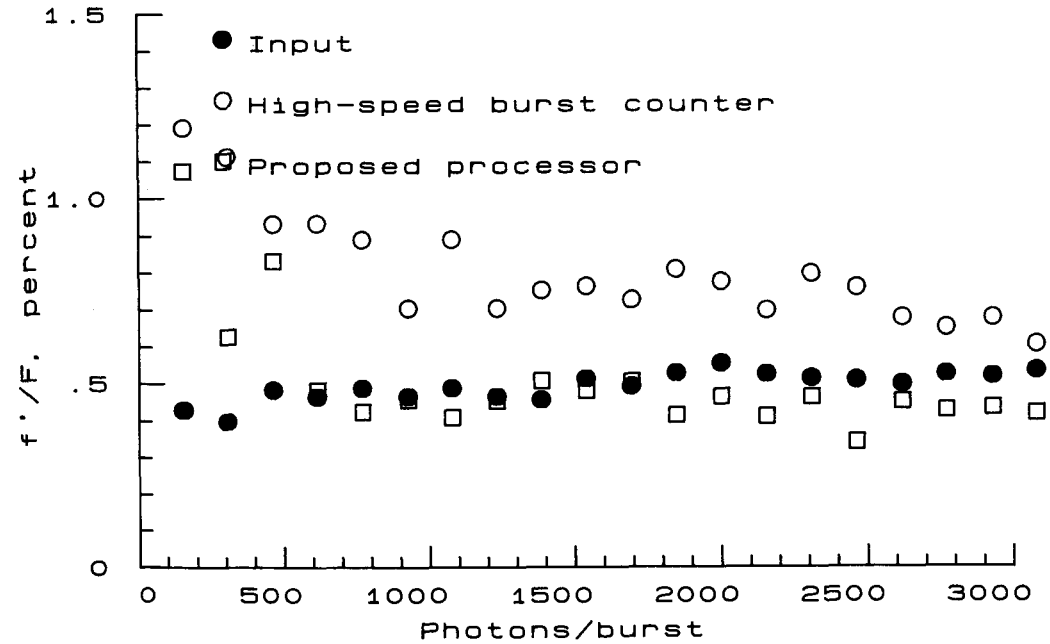

Figure 23. Simulation comparisons of input $f'/F = 0.5$ to measured f'/F for high-speed burst counter and frequency domain signal processor as a function of signal-to-noise ratio (photons/burst) at mean oscillation frequency of 25.0 MHz.

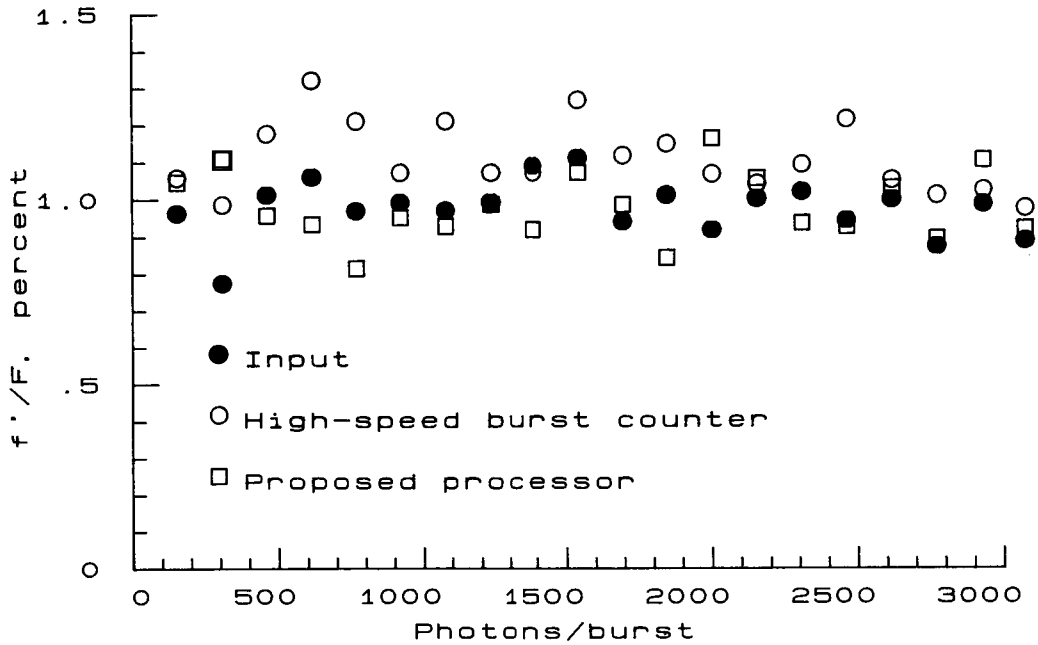

Figure 24. Simulation comparisons of input $f'/F = 1.0$ to measured f'/F for high-speed burst counter and the frequency domain signal processor as a function of signal-to-noise ratio (photons/burst) at mean oscillation frequency of 25.0 MHz.

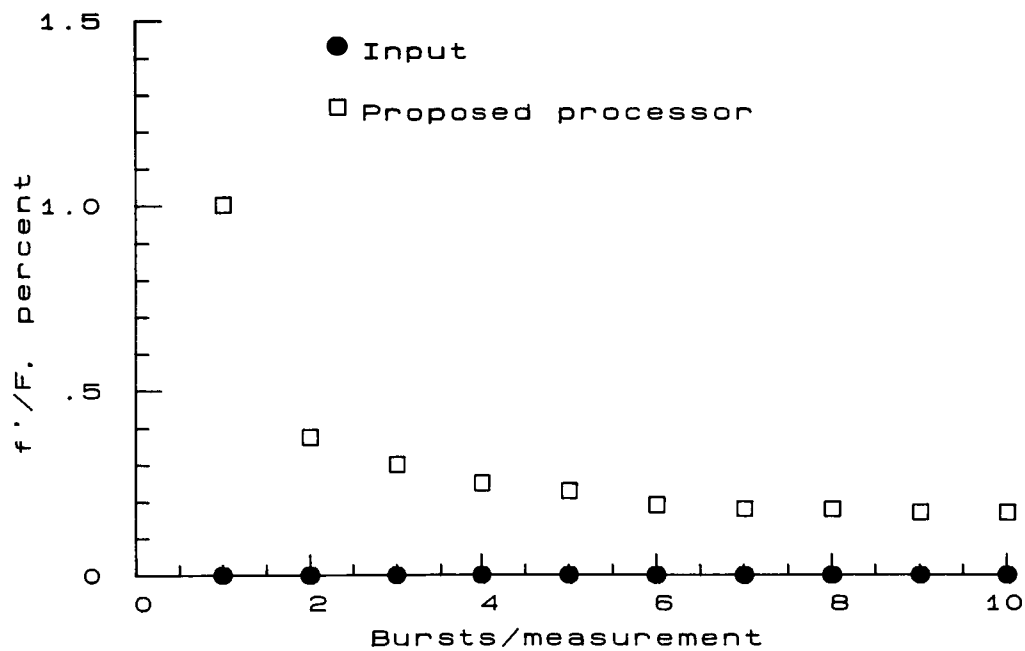

Figure 25. Simulation results of f'/F as a function of number of signal bursts per measurement by frequency domain signal processor for input f'/F of 0.0 and mean oscillation frequency of 25.0 MHz.

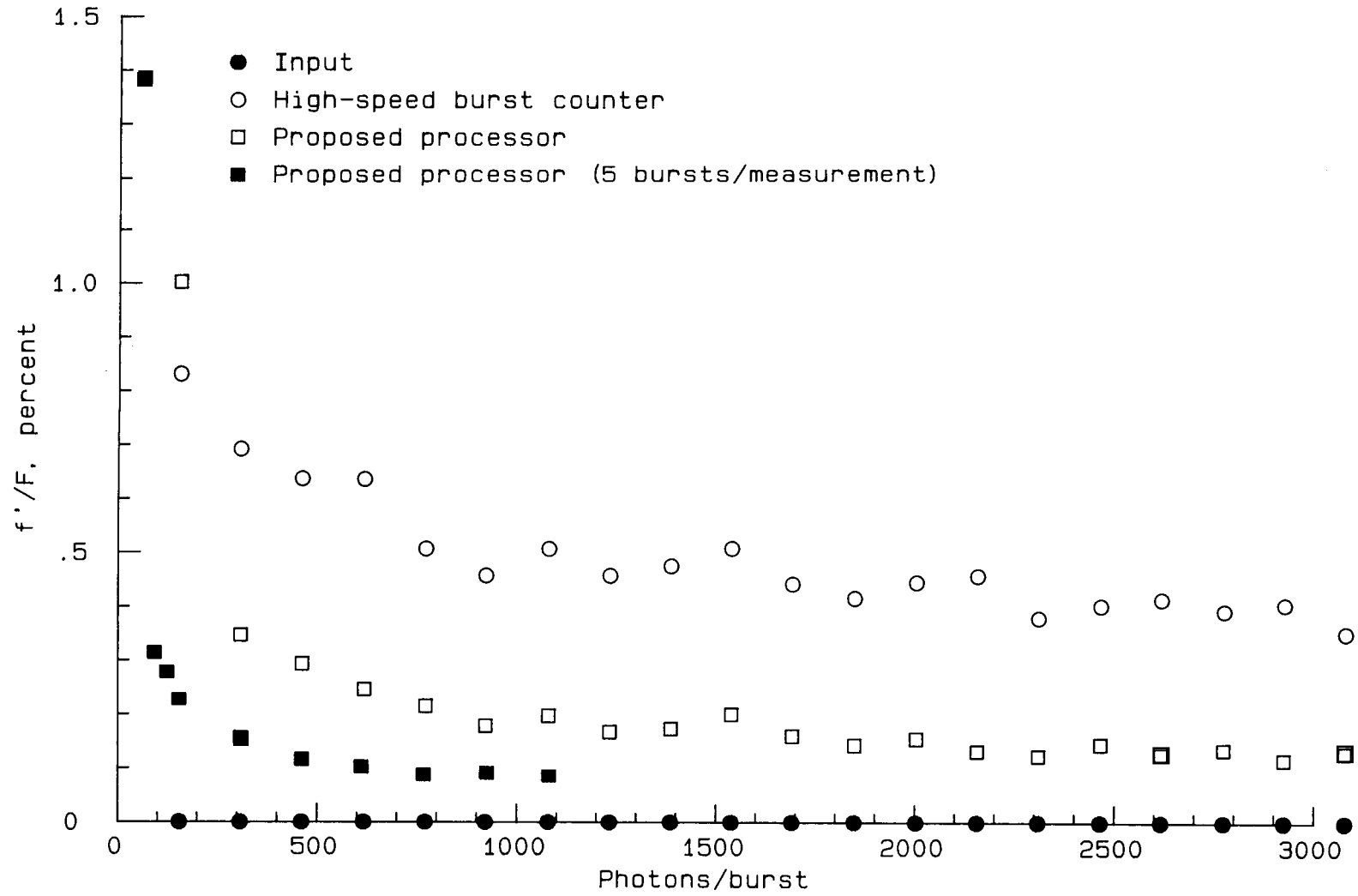

Figure 26. Simulation comparisons of input $f'/F = 0.0$ to measured f'/F for high-speed burst counter and frequency domain signal processor with single and multiple bursts per measurement as a function of signal-to-noise ratio (photons/burst) at mean oscillation frequency of 25.0 MHz.

NASA
National Aeronautics and Space Administration

Report Documentation Page

1. Report No.	2. Government Accession No.	3. Recipient's Catalog No.
NASA TP-2735		

4. Title and Subtitle	5. Report Date
Frequency Domain Laser Velocimeter Signal Processor— A New Signal Processing Scheme	September 1987
	6. Performing Organization Code
7. Author(s)	8. Performing Organization Report No.
James F. Meyers and James I. Clemmons, Jr.	L-16209
9. Performing Organization Name and Address	10. Work Unit No.
NASA Langley Research Center Hampton, VA 23665-5225	505-61-01-06
	11. Contract or Grant No.
12. Sponsoring Agency Name and Address	13. Type of Report and Period Covered
National Aeronautics and Space Administration Washington, DC 20546-0001	Technical Paper
	14. Sponsoring Agency Code

15. Supplementary Notes

16. Abstract

A new scheme for processing signals from laser velocimeter systems is described. The technique utilizes the capabilities of advanced digital electronics to yield a "smart" instrument that is able to configure itself, based on the characteristics of the input signals, for optimum measurement accuracy. The signal processor is composed of a high-speed 2-bit transient recorder for signal capture and a combination of adaptive digital filters with energy and/or zero crossing detection signal processing. The system is designed to accept signals with frequencies up to 100 MHz with standard deviations up to 20 percent of the average signal frequency. Results from comparative simulation studies indicate measurement accuracies 2.5 times better than with a high-speed burst counter, from signals with as few as 150 photons per burst.

17. Key Words (Suggested by Authors(s))	18. Distribution Statement
Laser velocimetry Laser anemometry Signal processing Laser applications	Unclassified—Unlimited Subject Category 36

19. Security Classif.(of this report)	20. Security Classif.(of this page)	21. No. of Pages	22. Price
Unclassified	Unclassified	37	A03

NASA FORM 1626 OCT 86 NASA-Langley, 1987

For sale by the National Technical Information Service, Springfield, Virginia 22161-2171